Journal Pre-proof

Synthesis, and biological evaluation of 3,6-diaryl-[1,2,4]triazolo[4,3-a]pyridine analogues as new potent tubulin polymerization inhibitors

Fang Yang, Xie-Er Jian, Peng-Cheng Diao, Xian-Sen Huo, Wen-Wei You, Pei-Liang Zhao

PII: S0223-5234(20)30597-3

DOI: https://doi.org/10.1016/j.ejmech.2020.112625

Reference: EJMECH 112625

To appear in: *European Journal of Medicinal Chemistry*

Received Date: 9 March 2020

Revised Date: 8 June 2020

Accepted Date: 25 June 2020

Please cite this article as: F. Yang, X.-E. Jian, P.-C. Diao, X.-S. Huo, W.-W. You, P.-L. Zhao, Synthesis, and biological evaluation of 3,6-diaryl-[1,2,4]triazolo[4,3-a]pyridine analogues as new potent tubulin polymerization inhibitors, *European Journal of Medicinal Chemistry*, https://doi.org/10.1016/j.ejmech.2020.112625.

Synthesis, and biological evaluation of 3,6-diaryl-[1,2,4]triazolo[4,3-a]pyridine analogues as new potent tubulin polymerization inhibitors

Fang Yang [1], Xie-Er Jian [1], Peng-Cheng Diao, Xian-Sen Huo, Wen-Wei You, Pei-Liang Zhao*

Guangdong Provincial Key Laboratory of New Drug Screening, School of Pharmaceutical Science, Southern Medical University, Guangzhou 510515, P.R.China

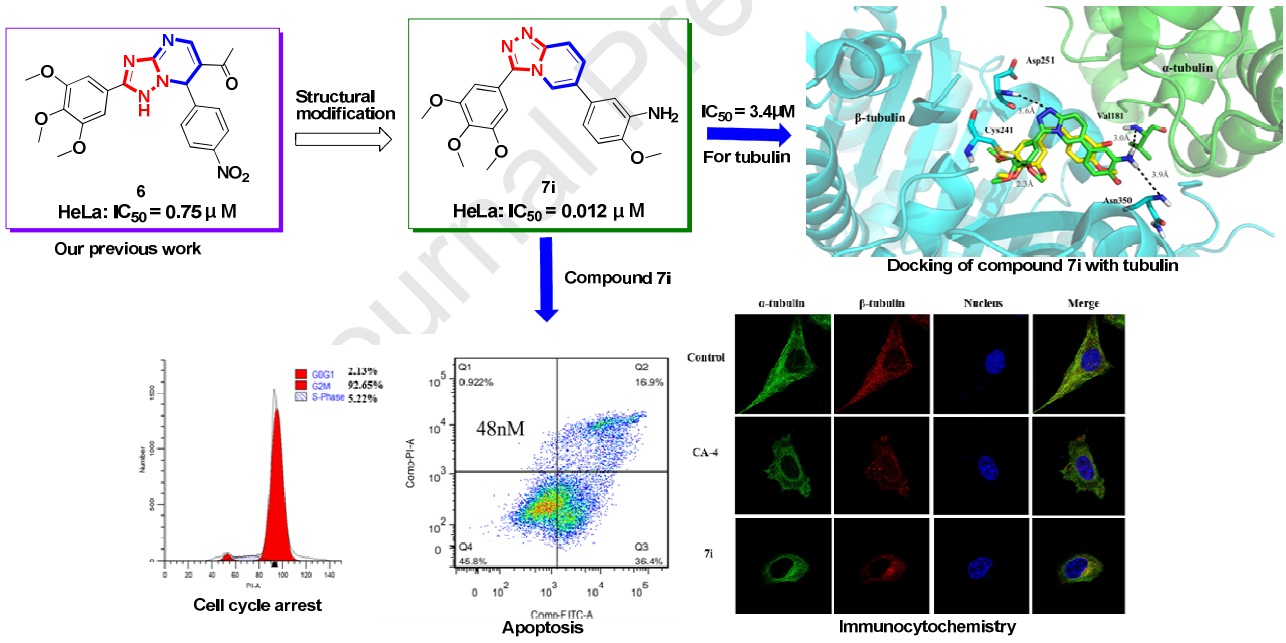

Synthesis, and biological evaluation of 3,6-diaryl-[1,2,4]triazolo[4,3-a]pyridine analogues as new potent tubulin polymerization inhibitors

Fang Yang [1], Xie-Er Jian [1], Peng-Cheng Diao, Xian-Sen Huo, Wen-Wei You, Pei-Liang Zhao*

Guangdong Provincial Key Laboratory of New Drug Screening, School of Pharmaceutical Science, Southern Medical University, Guangzhou 510515, P.R.China

ABSTRACT: On the basis of our previous work, twenty-nine novel [1,2,4]triazolo[4,3-a]pyridines possessing 3,4,5-trimethoxylphenyl groups were designed, synthesized, and evaluated as tubulin polymerization inhibitors. The bioassay results revealed that some of the compounds displayed excellent antiproliferative efficacies in the nanomolar range against HeLa cells, and the most promising derivative **7i** demonstrated almost comparable activity to that of the reference CA-4 and sixty-two fold more potent than the parent compound **6** with an IC_{50} value of 12 nM. Importantly, **7i** exhibited high selectivity over the normal human embryonic kidney HEK-293 cells (IC_{50} > 100 μM). Further mechanism studies revealed that **7i** significantly arrested cell cycle at G2/M phase, induced apoptosis with a dose-dependent manner, and disrupted microtubule networks. Additionally, the most active compound **7i** effectively inhibited tubulin polymerization with a value similar to that of CA-4 (3.4 and 4.2 μM, respectively). Furthermore, molecular docking analysis suggested that **7i** well occupied the colchicine binding pocket of tubulin. The present study highlights that compound **7i** is a novel potential tubulin polymerization inhibitor and deserves further investigation for the treatment of cancers.

Keywords: [1,2,4]Triazolo[4,3-a]pyridine; Synthesis; Antiproliferative activity; Tubulin polymerization.

*Corresponding author. E-mail address: plzhao@smu.edu.cn (P.-L. Zhao)

[1] These authors contributed equally to this work.

1. Introduction

Microtubules are one of the most successful therapeutic targets in tumour cells, and composed of α/β-tubulin dimmers, which provide a highly dynamic framework for maintaining cell structure, protein trafficking, and supporting the process of mitosis [1-3]. Microtubule-targeting agents were found to bind to be at least four different sites, among which inhibitors binding to the colchicine-site have been always attracting considerable attention in anti-cancer therapy due to their advantages such as simple structure, broad therapeutic index, and significant ability to overcome clinically relevant multidrug resistance [4-7].

In recent decades, a great deal of tubulin polymerization inhibitors with diverse backbones targeting the colchicines-site have been investigated [8-12]. Among them, 1,2,4-triazole fused heterocycles have recently drawn increasing interest as a privileged skeleton for the discovery of antitumor agents [13-16]. As shown in Fig. **1**, [1,2,4]triazole fused thiadiazole **1** displayed excellent antiproliferative activity on three cancer cell lines with IC_{50} values of 22–29 nM in the three cell lines [17]. Most interestingly, 1,2,4-triazole fused six-membered aromatic rings, presented as compounds **2** and **3**, exerted outstanding antitumor potencies in the low nanomolar range [18-19]. Recently, triazoloquinazolinone **4** has been developed as a significant tubulin polymerization inhibitor and vascular disrupting agent (Fig. **1**) [20].

Previously, we also reported a series of novel tubulin polymerization inhibitors, exampled by [1,2,4]triazolo[3,4-b][1,3,4]thiadiazine **5** and [1,2,4]triazolo[1,5-a]pyrimidine derivative **6** both bearing a 3,4,5-trimethoxyphenyl moiety [21-22], which is crucial for maintaining antiproliferative activities and is a common group shared by many colchicine-binding site inhibitors. On the other hand, pyridine ring is regarded as a privileged scaffold in medicinal chemistry and is frequently observed within a number of anticancer agents, particularly in the small-molecule tubulin inhibitors [23-26]. Inspired by the above considerations and in continuation of our efforts on optimizing the structure of the analogue **6**, we fused 1,2,4-triazole moiety with pyridine ring instead of pyrimidine core to generate compounds **7a**–**u** and **8a**–**h** which are also bioisosteres based on the [1,2,4]triazolo[4,3-b]pyridazine framework **2**. Herein, we described the detailed synthetic routes and their biological efficiency including antiproliferative activities, cytotoxicities toward a representative normal human cell line HEK-293, as well as their tubulin polymerization inhibitory

effects.

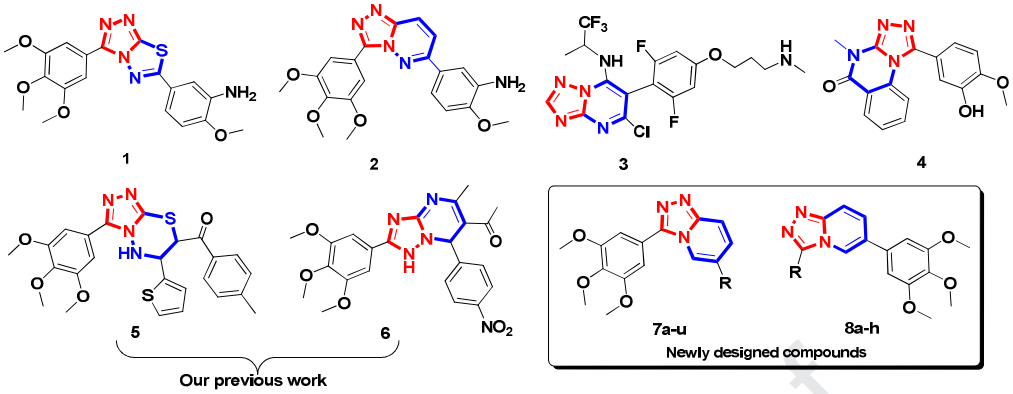

Fig. 1. Chemical structures of several representative tubulin inhibitors containing the 1,2,4-triazole fused heterocycle scaffold, and the general structure of target compounds **7a**–**u** and **8a**–**h**.

2. Chemistry

Synthesis of target compounds **7a**–**u** and **8a**–**h** was accomplished using a three-step procedure, respectively, illustrated in Scheme **1**. In brief, the condensation of commercially available 5-bromo-2-hydrazinylpyridine **9** with 3,4,5-trimethoxybenzaldehyde led to the formation of 3,4,5-trimethoxybenzylidenehydrazinyl substituted pyridine derivative **10** [27], which was cyclized into the corresponding key intermediate 6-bromo-3-phenyl-[1,2,4]triazolo[4,3-a]pyridine **11**. Subsequently, intermediate **11** was efficiently coupled with the appropriate arylboronic acids using a catalyst formed in situ from tris(dibenzylideneacetone)dipalladium and xantphos in the presence of K_3PO_4 in a mixed solution of DMSO/H_2O under N_2 atmosphere, and provided 3-(3,4,5-trimethoxyphenyl)-[1,2,4]triazolo[4,3-a]pyridine derivatives **7a**–**u** in yields ranging from 60 to 84%. Meanwhile, the designed target compounds **8a**–**h** bearing 3,4,5-trimethoxyphenyl moiety at C-6 position were also obtained from a three-step synthesis in a similar manner, starting from 5-bromo-2-hydrazinylpyridine **9** and various benzaldehydes. All target derivatives were fully characterized by ^{1}H NMR, ^{13}C NMR, and HRMS spectroscopic techniques, and purity of the most potent compound 7i was 97.05% based on HPLC analysis. The spectral data were in full agreement with the expected structures (see Experimental Section and Supporting Information).

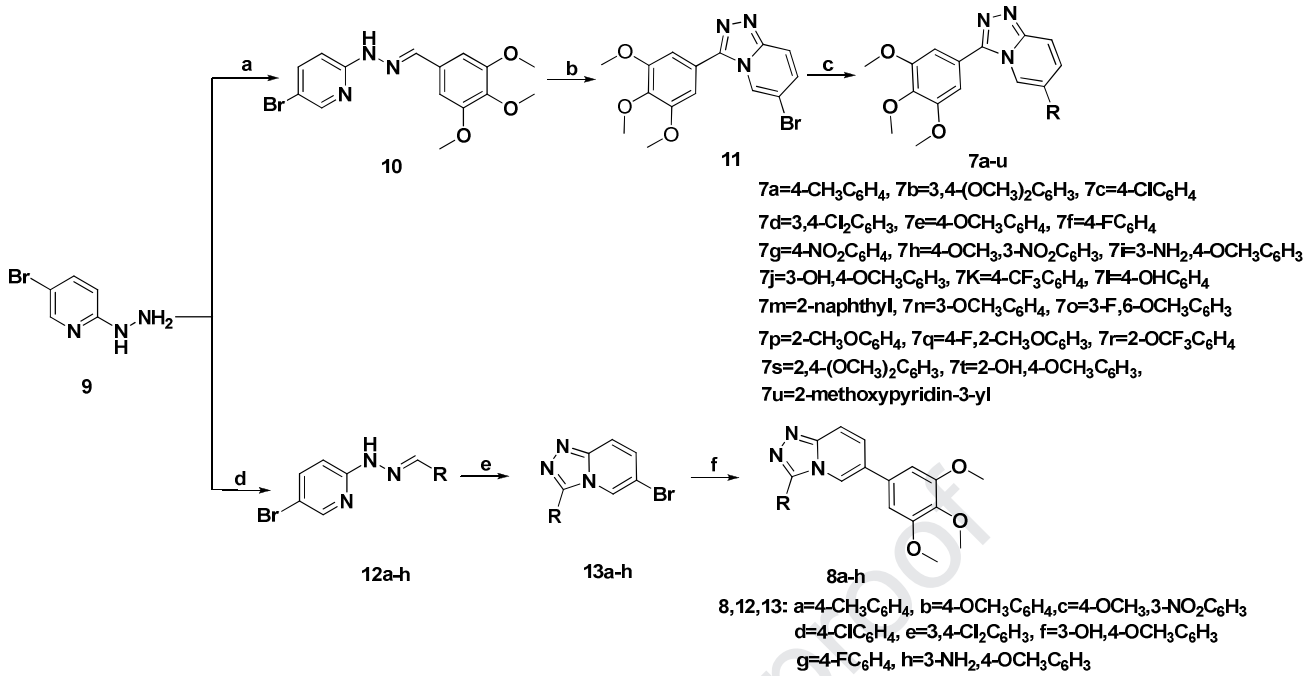

Scheme 1. Synthesis of the target compounds **7a**–**u** and **8a**–**h**. Reagents and conditions: (a) 3,4,5-trimethoxybenzaldehyde, ethanol, rt, 4h; (b) CH_2Cl_2, iodobenzene diacetate, N_2, rt, 10h; (c) DMF, H_2O, arylboronic acids, $Pd_2(dba)_3$, xantphos, K_3PO_4, N_2, 80 ^oC, 8-12h.; (d) substituted benzaldehyde, ethanol, rt, 3-5h; (e) CH_2Cl_2, iodobenzene diacetate, N_2, rt, 8-10h; (f) DMF, H_2O, (3,4,5-trimethoxyphenyl)boronic acid, $Pd_2(dba)_3$, xantphos, K_3PO_4, N_2, 80 ^oC, 8-12h.

3. Results and Discussion

3.1 In vitro antiproliferative activity

The *in vitro* antiproliferative efficacy of synthesized novel 1,2,4-triazolo[4,3-a]pyridine derivatives were first evaluated against human cervical cancer cells (HeLa), through 3-(4,5-dimethylthiazol-2-yl)-2,5-diphenyltetrazolium bromide (MTT) assay. The results expressed as IC_{50} (μM) were summarized in Table **1**, compared to our previously reported compound **6** and the reference Combretastatin A-4 (CA-4) which is a well-known tubulin inhibitor binding to the colchicine-site. Moreover, some highly active compounds were selected to futher explore their cytotoxic activity against a representative normal cell lines HEK-293 (human embryonic kidney cells). Here, the IC_{50} value represents the concentration of one compound resulting in a 50% inhibition in cell growth after 48 h incubation, and is the average of at least three independent

experiments.

As shown in Table **1**, generally, except for compounds **7k**–**m** and **7t**, nearly all of the tested derivatives **7a**–**u** with 3,4,5-trimethoxyphenyl at C-3 position of [1,2,4]triazolo[4,3-a]pyridine core demonstrated remarkable antiproliferative activities in a nanomolar range. In this series, fourteen analogues **7a**–**j** and **7n**–**q** displayed much more potent activities with IC_{50} values from 0.012 to 0.651 μM than our parent compound **6** (IC_{50} = 0.75 μM), but were still less active than that of CA-4 (IC_{50} = 4.7 nM). In particular, derivative **7i** featuring 3-amino-4-methoxyphenyl moiety, was found to be the most active compound with an IC_{50} value of 12 nM, which was approximately comparable with that of CA-4 and was almost sixty-two fold more potent than the lead analogue **6**, suggesting that the 3-(3,4,5-trimethoxyphenyl)-[1,2,4]triazolo[4,3-a]pyridine provides a useful skeleton for the development of anticancer agents. Interestingly, replacement of the 2-methoxy phenyl substituent (**7p**) by a 2-methoxypyridine group (**7u**) significantly decreased the antiproliferative activity. While substituting phenyl moiety with bulky naphthalenyl group, compound **7m** completely lost its inhibitory activity when compared to the **7a**–**l** and **7n**–**s**. However, all of the derivatives **8a**–**h**, which have 3,4,5-trimethoxyphenyl on the C-6 position of the core, always showed much lower activities than the corresponding analogus **7a**–**u** (for example, **8a** vs **7a**, **8b** vs **7e**, **8c** vs **7h**, **8d** vs **7c**, **8e** vs **7d**, **8f** vs **7j**, **8g** vs **7f**, **8h** vs **7i**), indicating that 3,4,5-trimethoxyphenyl on the C-3 position of fused-ring was critical for antiproliferative activity.

Most interestingly, all of the eight representative analogues **7a**, **7c**, **7f**–**j** and **7p** with potent antiproliferative efficacy did not exhibite inhibitory effect (IC_{50} > 100 μM) on the normal human embryonic kidney cells, HEK-293, while both the parent compound **6** and reference CA-4 displayed significant cytotoxicity with an IC_{50} value of 29.94, and 45.69 μM, respectively. The results manifested that these designed compounds might possess excellent selectivity over normal human cells, indicating a high safety index.

Table 1 Antiproliferative activities of derivatives **7a–u** and **8a–h** against HeLa cells, and cytotoxicity of some representative compounds.

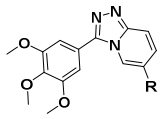

7a-u

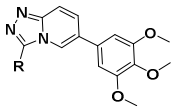

8a-h

Comp.	R	IC_{50} (μM)[a]		Comp	R	IC_{50} (μM)[a]	
		HeLa	HEK-293[b]			HeLa	HEK-293[b]
7a	4-$CH_3C_6H_4$	0.034±0.003	>100	**7q**	4-F,2-$OCH_3C_6H_3$	0.153±0.027	NT
7b	3,4-$(OCH_3)_2C_6H_3$	0.119±0.015	NT[c]	**7r**	2-$OCF_3C_6H_4$	22.19±1.32	NT
7c	4-ClC_6H_4	0.065±0.003	>100	**7s**	2,4-$(OCH_3)_2C_6H_3$	7.90±0.37	NT
7d	3,4-$Cl_2C_6H_3$	0.347±0.044	NT	**7t**	2-OH,4-$OCH_3C_6H_3$	>25	NT
7e	4-$OCH_3C_6H_4$	0.194±0.019	NT	**7u**		20.63±2.57	NT
7f	4-FC_6H_4	0.025±0.003	>100	**8a**	4-$CH_3C_6H_4$	>25	NT
7g	4-$NO_2C_6H_4$	0.023±0.002	>100	**8b**	4-$OCH_3C_6H_4$	>25	NT
7h	4-OCH_3,3-$NO_2C_6H_3$	0.062±0.007	>100	**8c**	4-OCH_3,3-$NO_2C_6H_3$	>25	NT
7i	3-NH_2,4-$OCH_3C_6H_3$	0.012±0.001	>100	**8d**	4-ClC_6H_4	>25	NT
7j	3-OH,4-$OCH_3C_6H_3$	0.045±0.007	>100	**8e**	3.4-$Cl_2C_6H_3$	>25	NT
7k	4-$CF_3C_6H_4$	>25	NT	**8f**	3-OH,4-$OCH_3C_6H_3$	22.09±1.30	NT
7l	4-OHC_6H_4	>25	NT	**8g**	4-FC_6H_4	>25	NT
7m		>25	NT	**8h**	3-NH_2,4-$OCH_3C_6H_3$	3.97±0.14	NT
7n	3-$OCH_3C_6H_4$	0.446±0.075	NT		**6**	0.75±0.02	29.94±0.69
7o	3-F,6-$OCH_3C_6H_3$	0.651±0.082	NT		**CA-4**	0.0047±0.0002	45.69 ± 5.15
7p	2-$OCH_3C_6H_4$	0.084±0.015	>100				

[a] 50% inhibitory concentration and mean ± SD of at least three independent experiments performed in duplicate.

[b] Normal human embryonic kidney (HEK-293) cell lines.

[c] NT: not tested.

Moreover, some potent analogues with excellent antiproliferative activity on HeLa were further tested against three additional different cancer cell lines, including human lung adenocarcinoma cell line (A549), and human breast cell line (MCF-7 and T47D), and were also compared with the reference compound CA-4. The results are presented in Table **2**, which revealed some representative compounds effectively inhibited the proliferation of a variety of cancer types.

Among them, **7i** was found to be the most active analogue, and exhibited potent activities against A549, MCF-7, and T47D, suggesting that **7i** could be a potential anticancer agent worthy of further investigation.

Table 2 Antiproliferative activities of representative compounds against three cancer cell lines.

Compd.	R	IC_{50} (μM)		
		A549	MCF-7	T47D
7a	4-$CH_3C_6H_4$	6.26±0.91	>100	>100
7b	3,4-$(OCH_3)_2C_6H_3$	87.08±0.94	>100	>100
7f	4-FC6H4	78.62±4.10	>100	75.97±0.96
7h	4-OCH_3,3-$NO_2C_6H_3$	58.67±1.08	75.71±0.83	>100
7i	3-NH_2,4-$OCH_3C_6H_3$	10.40±2.17	40.40±6.17	27.91±3.22
7j	3-OH,4-$OCH_3C_6H_3$	17.76±3.04	>100	>100
7p	2-$OCH_3C_6H_4$	9.28±0.81	13.69±2.779	31.54±2.05
CA-4	\	0.021±0.04	0.17±0.07	0.0019±0.0003

[a]IC_{50} is the concentration of compound required to decrease cell growth by 50% and values reported represent the mean ± SD (standard deviation) of three independent experiments.

3.2. Cell cycle analysis

Encouraged by the preliminary antiproliferative screening results, the anticancer mechanism of these compounds was further explored, and the most promising analogue **7i** was selected to examine the influence on the cell cycle. In this study, HeLa cells were incubated with increased concentrations of **7i** (12, 24, and 48 nM) for 24 h. As illustrated in Fig. **2**, the percentage of cells at the G2/M phase in presence of the compound was 13.90%, 26.00%, and 92.65%, respectively, while 11.14% of G2/M phase was detected for the control group. These findings demonstrated that compound **7i** caused a clear G2/M arrest pattern in a concentration-dependent manner.

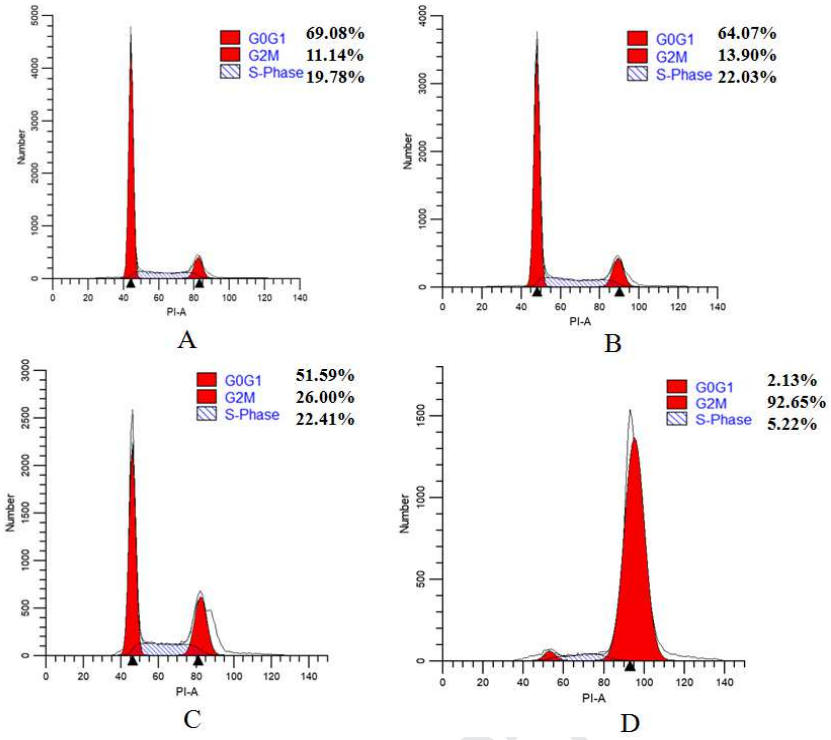

Fig. 2. Effect of compound **7i** on cell cycle in HeLa cells. Flow cytometry of HeLa cells treated with **7i** for 24h. (A) Control; (B) **7i**, 12 nM; (C) **7i**, 24 nM; (D) **7i**, 48 nM.

It has been known mitosis promoting factor formed between cdc2 and cyclin B1, plays a key role during the transition from interphase to mitotic phase and controls cell cycle progression through increasing distribution in the G2/M phase [28-29]. Hence, we studied alterations in expression of cell cycle regulatory proteins to achieve insight into the mechanism of **7i**-induced G2/M arrest in HeLa. As presented in Figure **3**, **7i** concentration-dependently decreased cyclin B1 and cdc2 protein levels, which indicated that **7i**-caused G2/M arrest might be correlated with the alterations of expression of cyclin B1 and cdc2.

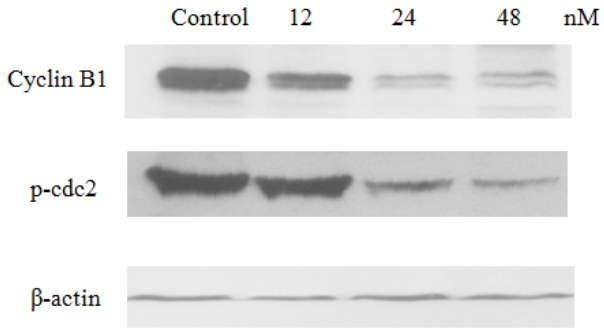

Figure **3**. Effects of **7i** on G2/M regulatory proteins. HeLa cells were treated for 24 h with the indicated concentration of **7i** (12, 24 and 48 nM). The cells were harvested and lysed for the detection of cyclin B1 and

p-cdc2.

3.3. Cell apoptosis study

In order to investigate the mode of cell death produced by **7i**, cell apoptosis analysis of HeLa cells incubated with the increasing concentrations of the compound was performed using an Annexin V-FITC/PI assay. As shown in Fig. **4**, when the cells were incubated with **7i** at 12, 24, and 48 nM for 24 h, the total numbers of early and late apoptotic cells were 8.44%, 26.87% and 53.3%, respectively, whereas that of control group was only 6.31%. Therefore, these results indicated that compound **7i** effectively induced cell apoptosis in HeLa cells via a dose-dependent manner.

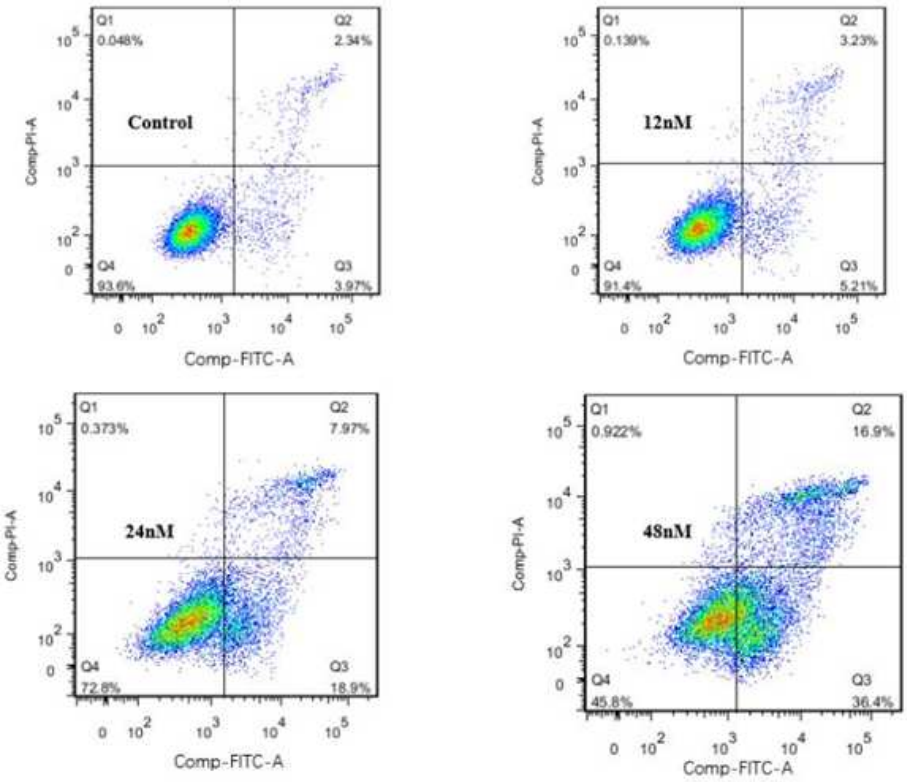

Fig. 4. Flow cytometric analysis of apoptotic cells after treatment of HeLa cells with derivative **7i** at different concentrations (12, 24, 48 nM) and no treatment (control) as a reference control for 24 h. The lower left quadrant represents live cells, the lower right stands for early apoptotic cells, the upper right represents late apoptotic cells and the upper left is for cells necrosis.

Activation of caspase-3 plays a vital role for the initiation and execution of the apoptotic process. Among the caspase-3, PARP cleavage, an essential indicator of apoptosis induction, is a

key indicator of caspase-3 activation. Hence, in order to understand the correlation of antiproliferative activity with cellular death by apoptosis by these analogues, we examined the activation of caspase-3 in HeLa cells exposed to compound **7i** (12, 24 and 48 nM). Results indicated that a significant increase in the levels of cleaved PARP was observed by treatment with **7i** for 24 h via a concentration-dependent manner (Fig. **5**), suggesting that **7i** induced apoptosis in cancer cells by activation of caspase-3. Additionally, in this study, it was clear that the important anti-apoptotic protein Bcl-2 was down regulated after 24 h of treatment compare to the control, which revealed that the induction of apoptosis by **7i** is associated with Bcl-2 down-regulation.

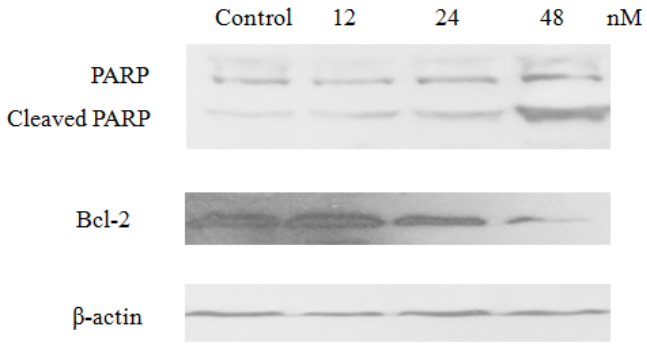

Fig. 5. Western blotting analysis of the expression of cleaved PARP and Bcl-2. HeLa cells were treated for 24 h with the indicated concentration of **7i** (12, 24 and 48 nM). Cell lysates were collected, and the expression levels of PARP and Bcl-2 were determined by western blot analysis. β-actin was used as a loading control.

3.4. In vitro tubulin polymerization assay

To examine whether microtubule system could be a potential target of these compounds, the above seven highly active derivatives 7**a**, **7b**, **7f**, 7**h**, **7i**, **7j**, and **7p** were initially chose to evaluate their *in vitro* tubulin polymerization inhibition at the concentration of 10 μM, comparing to the reference tubulin polymerization inhibitor CA-4. As shown in Table **3**, most of the tested compounds significantly inhibited tubulin polymerization. Particularly, compounds **7a**, **7b**, and **7i** inhibited tubulin polymerization by 77, 68 and 81 %, respectively, while 79 % inhibition was

observed with CA-4. Further screening revealed that **7i** (Fig. **6**), the most potent analogue on HeLa cells, also exhibited much higher anti-tubulin activity than CA-4 (IC_{50} = 4.2 μM) with an IC_{50} value of 3.4 μM. These results suggested that influence on the tubulin polymerization inhibition correlated well with their antiproliferative efficacy, and tubulin was the most likely the target of these compounds.

Table 3 Tubulin polymerization inhibitory activities of the most potent compounds

Comp.	R	Tubulin polymerization	
		%inhibition[a]	IC_{50}(μM)[b]
7a	4-$CH_3C_6H_4$	77	4.1±0.1
7b	3.4-$(OCH_3)_2C_6H_3$	68	11.3±1.0
7f	4-FC_6H_4	18	NT[c]
7h	4-OCH_3,3-$NO_2C_6H_3$	36	NT
7i	3-NH_2,4-$OCH_3C_6H_3$	81	3.4±0.1
7j	3-OH,4-$OCH_3C_6H_3$	14	NT
7p	2-$OCH_3C_6H_4$	16	NT
CA-4		79	4.2±0.1

[a] Compounds were tested at a final concentration of 10μM.

[b] IC_{50} values are presented as mean values of three independent experiments done in quadruplicates.

[c] NT: Not test.

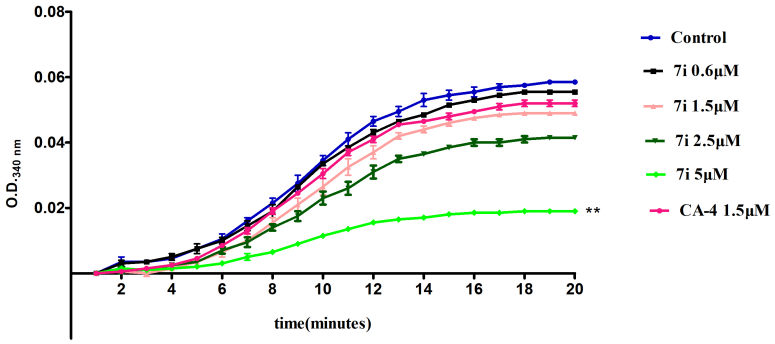

Fig. 6. Effects of **7i** on tubulin polymerization *in vitro*. Tubulin in reaction buffer was incubated at 37°C in the presence of the control (1% DMSO), compound **7i** (0.6, 1.5, 2.5, 5 μM) or the reference CA-4 (1.5 μM). Absorbance at 340 nm was monitored at 37 °C every minute, and polymerizations were followed by an increase in

fluorescence emission at 340 nm over a 20 min period. Data are presented as the mean ± SD from three independent experiments. $^{**}P < 0.01$ vs the vehicle control.

3.5. Immunocytochemistry

To substantiate the direct effects of these analogus on tubulin, immunohistochemistry was carried out to investigate alterations in the microtubule network caused by compound **7i** in cultured HeLa cells, compared with that of CA-4 at the same level of concentration. As depicted in Fig. **7**, the microtubule network exhibited normal arrangement and organization in the untreated HeLa cells. Whereas, exposure to 12 nM of **7i** for 6h led to significantly disrupt microtubule organization, which was similar to those of CA-4. These results indicated that compound **7i** showed similar effects to CA-4 on the microtubule network and thus revealed that **7i** inhibited the tubulin polymerization.

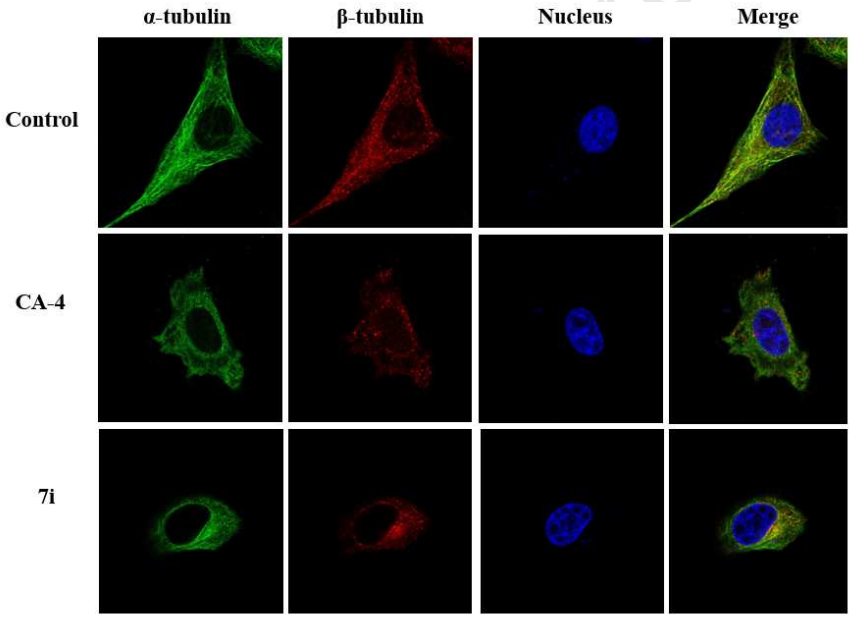

Fig. 7. Compound **7i** and CA-4 induced microtubules depolymerization in HeLa cells. HeLa cells were processed with **7i** and CA-4 at 12 nM concentration for 6h, followed by immunofluorescent staining with anti-α-tubulin antibody (green), anti-β-tubulin antibody (red) and DIPA (blue, for nuclear staining). Images were captured with laser scanning confocal microscope.

3.6. Molecular studies

In order to illustrate the possible binding mode, the most active compound **7i** was chose to perform the molecular docking simulations on the colchicine-site of tubulin. As given in Fig. **8**, **7i** and CA-4 adopted quite similar location at the colchicine binding pocket in the co-crystallized tubulin structure (PDB: 5lyj). The triazolopyridine core of the **7i** was extended deeply in the *β*-subunit of the tubulin and the N-1 of the triazole ring formed a hydrogen-bonding interaction with

residue *β*-Asp251. Meanwhile, the much stronger hydrogen bond existed between the oxygen atom of 3,4,5-trimethoxylphenyl moiety and the residue *β*-Cys241 which was consistent with that of the 4-methoxyl group of CA-4. Furthermore, the 3-amino moiety of phenyl ring established two additional hydrogen bonds with *α*-Val181 and *β*-Asn350. The docking studies further indicated that compound **7i** may be a potential tubulin inhibitor binding to the colchicine site.

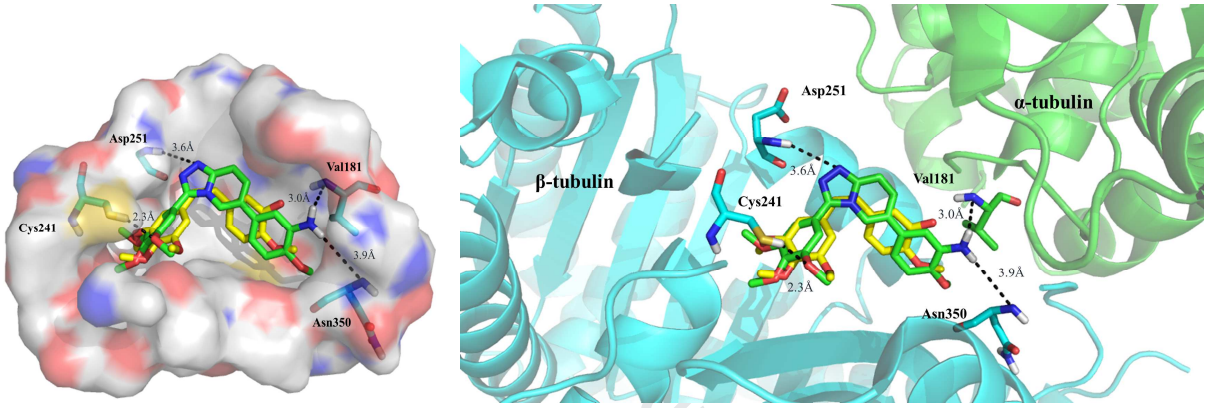

Fig. 8. Proposed binding model for **7i** (green stick) overlaid with CA-4 (yellow stick) in colchicine-site of tubulin (PDB code: 5lyj). The main interacting residues are shown and labeled. The black dashed lines were the potential H-bond between Cys241 (2.3Å), Val181 (3.0Å), Asp251 (3.6Å), Asn350 (3.9Å). Final figure for docking pose was generated by PyMOL.

4. Conclusion

On the basis of our previous work, a series of novel 3,4,5-trimethoxyphenyl substituted [1,2,4]triazolo[4,3-a]pyridines were designed and synthesized with a triazolopyrimidine **6** as the parent compound. Some target compounds exhibited improved antiproliferative efficacy in a nanomolar range against HeLa cells, and the most promising derivative **7i** displayed excellent antiproliferative efficacy with an IC_{50} value of 12 nM, which was approximately comparable to that of the reference CA-4, and was almost sixty-two fold more potent than the analogue **6**. The results indicated that the bioisosteric replacement of the pyrimidine moiety of triazolo[4,3-a]pyrimidine with a pyridine ring successfully enhanced potent activity. Most interestingly, **7i** exhibited outstanding selectivity over the normal human embryonic kidney HEK-293 cells (IC_{50} > 100 μM), which manifested that the compound might have much lower toxicity. Further mechanistic studies demonstrated that **7i** significantly arrested cell cycle at G2/M phase, induced apoptosis with a dose-dependent manner, and also disrupted microtubule networks. In addition, tubulin

polymerization assay suggested that analogue **7i** manifested much higher anti-tubulin activity than CA-4. Furthermore, molecular docking studies revealed that **7i** well occupied the colchicine-site in a similar way with CA-4. The preliminary observations highlight that compound **7i** is a novel potential tubulin polymerization inhibitor and deserves further investigation for the treatment of cancers.

5. Experimental protocols

5.1 Chemistry

Melting points were measured on a Buchi B-545 melting point apparatus and uncorrected. ^{1}H and ^{13}C NMR spectra were determined on a Mercury-Plus 400 spectrometer in $CDCl_3$ or DMSO-d_6 solution at room temperature, and chemical shift (δ) was expressed in parts per million (ppm) using TMS as an internal standard. High-resolution mass spectra (HRMS) performed on an Agilent QTOF 6540 mass spectrometer. Unless otherwise noted, all of chemicals were purchased from commercial suppliers and used without further purification.

*5.2 General procedure for the preparation of derivatives **7a**–**u** and **8a**–**h**.*

*5.2.1. General procedure for the preparation of the **7a**–**u**.*

*(E)-5-bromo-2-(2-(3,4,5-trimethoxybenzylidene)hydrazinyl)pyridine **10**.*

A solution of 5-bromo-2-hydrazinylpyridine **8** (2.2 g, 10mmol) in ethanol (80 mL) was added to 3,4,5-trimethoxybenzaldehyde (2.0 g, 10 mmol) and the resulting mixture was stirred for 4 h at room temperature. The crude product was then filtered, washed with ethanol (10 mL× 3) and dried to give compound **10** as a solid in the yield of 91%, which was used for next step reaction without purification.

*6-bromo-3-(3,4,5-trimethoxyphenyl)-[1,2,4]triazolo[4,3-a]pyridine **11**.*

To the solution of **10** (5 mmol) in DCM (80 mL) was added iodobenzene diacetate (5 mmol) at room temperature under nitrogen atmosphere. The resulting mixture was stirred for 10 h, poured into water, and extracted with ethyl acetate (80 mL×3). The solvents were then removed in vacuo, and the solid was filtered off, washed with methanol (3 mL ×2) and dried to afford **11**.

6-Bromo-3-(3,4,5-trimethoxy-phenyl)-[1,2,4]triazolo[4,3-a]pyridine. Yield, 83%; mp: 223.4–225.1°C; ^{1}H NMR (400 MHz, $CDCl_3$) δ: 3.95 (s, 6H, 2×CH_3O), 3.96 (s, 3H, CH_3O), 7.07 (s,

2H, Ph-H), 7.59 (d, *J* = 9.2 Hz, 1H, Pyridine-H), 7.91 (d, *J* = 9.2 Hz, 1H, Pyridine-H), 8.44 (s, 1H, Pyridine-H). ^{13}C NMR (100 MHz, $CDCl_3$) δ: 153.74, 150.46, 147.58, 137.94, 133.45, 129.32, 128.06, 126.81, 123.86, 105.25, 60.62, 56.88.

*General procedure for the preparation of the **7a**–**u**.*

A mixture of **11** (0.40 mmol), $Pd_2(dba)_3$ (0.04 mmol), xantphos (0.05 mmol), K_3PO_4 (0.48 mmol) and substituted arylboronic acids (0.41 mmol) in DMF/H_2O (20 mL, 5:1) was degassed and purged with N_2 for about three times. After stirred at 80°C for about 8-12 h (indicated by TLC) under N_2 atmosphere, the reaction mixture was poured into H_2O (50 mL) and extracted with ethyl acetate (80 mL×3). The combined organics were washed with brine (10 mL×3), dried over anhydrous Na_2SO_4, filtered and concentrated under vacuum to give a residue, which was purified by column chromatography using a mixture of petroleum ether and acetone (3:1) as an eluent to provide the target compounds **7a**–**u** in yields of 60–84%.

*5.2.1.1. 6-p-Tolyl-3-(3,4,5-trimethoxyphenyl)-[1,2,4]triazolo[4,3-a]pyridine (**7a**).* Yield, 80%; mp: 184.7–185.9°C; ^{1}H NMR (400 MHz, $CDCl_3$) δ: 2.43 (s, 3H, CH_3), 3.95 (s, 6H, 2×CH_3O), 3.96 (s,3H, CH_3O), 7.07 (s, 2H, Ph-H), 7.31 (d, *J* = 8 Hz, 2H, Ph-H), 7.44 (d, *J* = 8 Hz, 2H, Ph-H), 7.57 (d, *J* = 9.2 Hz, 1H, Pyridine-H), 7.88 (d, *J* = 9.2 Hz, 1H, Pyridine-H), 8.39 (s, 1H, Pyridine-H). ^{13}C NMR (100 MHz, $CDCl_3$) δ: 153.96, 149.85, 146.93, 139.81, 138.68, 133.25, 130.01, 128.78, 128.39, 126.73, 121.85, 118.88, 116.52, 105.81, 60.97, 56.46, 21.10. HRMS (ESI) *m/z*: calcd for $C_{22}H_{21}N_3O_3$ ($M+H^+$) 376.1656 found 376.1645.

*5.2.1.2. 6-(3,4-Dimethoxyphenyl)-3-(3,4,5-trimethoxyphenyl)-[1,2,4]triazolo[4,3-a]pyridine (**7b**).* Yield, 81%; mp: 101.9–102.2°C; ^{1}H NMR (400 MHz, $CDCl_3$) δ: 3.78 (s, 3H, CH_3O), 3.81 (s, 3H, CH_3O), 3.85 (s,3H, CH_3O), 3.90 (s,6H, 2×CH_3O), 7.07 (d, *J* = 8.4 Hz, 1H, Ph-H), 7.28 (s, 2H, Ph-H), 7.30 (s, 1H, Ph-H), 7.36 (s, 1H, Ph-H), 7.80 (d, *J* = 9.6 Hz, 1H, pyridine), 7.93 (d, *J* = 9.6 Hz, 1H, pyridine), 8.66 (s, 1H, pyridine). ^{13}C NMR (100 MHz, DMSO-d_6) δ: 153.89, 149.67, 149.55, 149.50, 146.82, 139.23, 129.00, 128.82, 127.55, 122.34, 120.28, 119.81, 115.80, 112.62, 111.21, 106.22, 60.55, 56.61, 56.01, 55.97. HRMS (ESI) *m/z*: calcd for $C_{23}H_{23}N_3O_5$ ($M+H^+$) 422.1710 found 422.1701.

*5.2.1.3. 6-(4-Chlorophenyl)-3-(3,4,5-trimethoxyphenyl)-[1,2,4]triazolo[4,3-a]pyridine (**7c**).* Yield, 78%; mp: 166.7–168.5; ^{1}H NMR (400 MHz, DMSO-d_6) δ: 3.78 (s, 3H, CH_3O), 3.88 (s, 6H, 2×CH_3O), 7.24 (s, 2H, Ph-H), 7.56 (d, *J* = 8.4 Hz, 2H, Ph-H), 7.80 (m, 3H, Ph-H, Pyridine-H), 7.96 (d, *J* = 9.2 Hz, 1H, Pyridine-H), 8.69 (s, 1H, Pyridine-H). ^{13}C NMR (100 MHz, $CDCl_3$) δ: 154.02, 149.75, 147.08, 139.96, 134.89, 134.66, 129.54, 128.17, 127.91, 127.74, 121.64, 119.34, 116.89,

105.87, 60.98, 56.49. HRMS (ESI) *m/z*: calcd for $C_{21}H_{18}ClN_3O_3$ ($M+H^+$) 396.1109 found 396.1103.

*5.2.1.4. 6-(3,4-Dichlorophenyl)-3-(3,4,5-trimethoxyphenyl)-[1,2,4]triazolo[4,3-a]pyridine (**7d**).* Yield, 79%; mp: 194.4–195.0°C; ^{1}H NMR (400 MHz, $CDCl_3$) δ: 3.95 (s, 6H, 2×CH_3O), 3.97 (s, 3H, CH_3O), 7.04 (s, 2H, Ph-H), 7.39 (dd, J_1 = 1.6 Hz, J_2 = 8 Hz, 1H, Ph-H), 7.49 (d, J = 9.6 Hz, 1H, Pyridine-H), 7.58 (d, J = 8.4 Hz, 1H, Ph-H), 7.64 (s, 1H, Ph-H), 7.91 (d, J = 9.6 Hz, 1H, Pyridine-H), 8.39 (s, 1H, Pyridine-H). ^{13}C NMR (100 MHz, $CDCl_3$) δ: 154.05, 149.67, 147.19, 140.05, 136.19, 133.59, 133.08, 131.29, 128.84, 127.49, 126.65, 126.11, 121.45, 119.72, 117.13, 105.88, 60.98, 56.49. HRMS (ESI) *m/z*: calcd for $C_{21}H_{17}Cl_2N_3O_3$ ($M+H^+$) 430.0720 found 430. 0719.

*5.2.1.5. 6-(4-Methoxyphenyl)-3-(3,4,5-trimethoxyphenyl)-[1,2,4]triazolo[4,3-a]pyridine (**7e**).* Yield, 81%; mp: 184.3–186.0°C; ^{1}H NMR (400 MHz, $CDCl_3$) δ: 3.88 (s, 3H, CH_3O), 3.96 (s, 6H, 2×CH_3O), 3.97 (s,3H, CH_3O), 7.04 (d, J = 8.4 Hz, 2H, Ph-H), 7.07 (s, 2H, Ph-H), 7.48 (d, J = 8.4 Hz, 2H, Ph-H), 7.55 (d, J = 9.6 Hz, 1H, Pyridine-H), 7.89 (d, J = 9.6 Hz, 2H, Pyridine-H), 8.36 (s, 1H, Pyridine-H). ^{13}C NMR (100 MHz, $CDCl_3$) δ: 160.07, 153.97, 149.79, 146.90, 139.83, 128.52, 128.50, 128.38, 128.05, 121.89, 118.44, 116.51, 114.76, 105.85, 60.98, 56.48, 55.38. HRMS (ESI) *m/z*: calcd for $C_{22}H_{21}N_3O_4$ ($M+H^+$) 392.1605 found 392.1604.

*5.2.1.6. 6-(4-Fluorophenyl)-3-(3,4,5-trimethoxyphenyl)-[1,2,4]triazolo[4,3-a]pyridine (**7f**).* Yield, 75%; mp: 186.6–186.8°C; ^{1}H NMR (400 MHz, DMSO-d_6) δ: 3.78 (s, 3H, CH_3O), 3.89 (s, 3H, 2×CH_3O), 7.24 (s, 2H, Ph-H), 7.34 (t, J_1 = 8.8 Hz, J_2 = 17.6 Hz, 2H, Ph-H), 7.77 (d, J = 9.6 Hz, 1H, Pyridine-H), 7.83 (dd, J_1 = 5.6 Hz, J_2 = 8.4 Hz, 2H, Ph-H), 7.95 (d, J = 9.6 Hz, 1H, Pyridine-H), 8.65 (s, 1H, Pyridine-H). ^{13}C NMR (100 MHz, DMSO-d_6) δ: 162.68 (d, J = 243.8 Hz, 1C), 153.87, 149.59, 147.05, 139.29, 132.76 (d, J = 2.9 Hz, 1C), 129.70 (d, J = 8.2 Hz, 2C), 128.77, 126.54, 122.21, 121.11, 116.34 (d, J = 21.5 Hz, 2C), 116.00, 106.47, 60.53, 56.66. HRMS (ESI) *m/z*: calcd for $C_{21}H_{18}FN_3O_3$ ($M+H^+$) 380.1405 found 380.1399.

*5.2.1.7. 6-(4-Nitrophenyl)-3-(3,4,5-trimethoxyphenyl)-[1,2,4]triazolo[4,3-a]pyridine (**7g**).* Yield, 84%; mp: 172.5–173.3°C; ^{1}H NMR (400 MHz, $CDCl_3$) δ: 3.95 (s, 6H, 2×CH_3O), 3.97 (s, 3H, CH_3O), 7.05 (s, 2H, Ph-H), 7.58 (d, J = 9.6 Hz, 1H, Pyridine-H), 7.74 (d, J = 8.4 Hz, 2H, Ph-H), 7.97 (d, J = 9.6 Hz, 1H, Pyridine-H), 8.37 (d, J = 8.8 Hz, 2H, Ph-H), 8.49 (s, 1H, Pyridine-H). ^{13}C NMR (100 MHz, $CDCl_3$) δ: 154.10, 149.67, 147.85, 147.37, 142.55, 140.17, 127.77, 127.26, 126.67, 124.59, 121.31, 120.54, 117.43, 105.96, 61.00, 56.54. HRMS (ESI) *m/z*: calcd for $C_{21}H_{18}N_4O_5$ ($M+H^+$) 407.1350 found 407.1345.

*5.2.1.8. 6-(4-Methoxy-3-nitrophenyl)-3-(3,4,5-trimethoxyphenyl)-[1,2,4]triazolo[4,3-a]pyridine (**7h**).* Yield, 75%; mp: 181.7–182.4°C; ^{1}H NMR (400 MHz, $CDCl_3$) δ: 3.96 (s, 6H, 2×CH_3O), 3.98 (s, 3H, CH_3O), 4.05 (s,3H, CH_3O), 7.06 (s, 2H, Ph-H), 7.26 (d, J = 8.8 Hz, 1H, Ph-H), 7.53 (d, J =

9.6 Hz, 1H, Pyridine-H), 7.75 (t, J_1 = 2 Hz, J_2 = 8.4 Hz, 1H, Ph-H), 7.94 (d, J = 9.6 Hz, 1H, Pyridine-H), 8.07 (d, J = 2 Hz, 1H, Ph-H), 8.42 (s, 1H, Pyridine-H). ^{13}C NMR (100 MHz, $CDCl_3$) δ: 154.06, 153.17, 149.61, 147.16, 140.02, 139.89, 132.34, 128.63, 127.45, 126.36, 124.18, 121.43, 119.46, 117.17, 114.55, 105.82, 60.98, 56.77, 56.47. HRMS (ESI) *m/z*: calcd for $C_{22}H_{20}N_4O_6$ ($M+H^+$) 437.1456 found 437.1464.

5.2.1.9. 2-Methoxy-5-(3-(3,4,5-trimethoxyphenyl)-[1,2,4]triazolo[4,3-a]pyridin-6-yl)aniline ***(7i)****.* Yield, 62%; mp: 195.1–195.5°C; ^{1}H NMR (400 MHz, $CDCl_3$) δ: 3.92 (s, 3H, CH_3O), 3.95 (s, 6H, 2×CH_3O), 3.97 (s, 3H, CH_3O), 6.89 (s, 3H, Ph-H), 7.06 (s, 2H, Ph-H), 7.53 (d, J = 9.2 Hz, 1H, Pyridine-H), 7.85 (d, J = 9.6 Hz, 1H, Pyridine-H), 8.33 (s, 1H, Pyridine-H). ^{13}C NMR (150 MHz, $CDCl_3$) δ: 153.99, 149.90, 147.77, 146.89, 139.79, 137.04, 129.06, 129.05, 128.71, 121.99, 118.43, 116.91, 116.27, 113.00, 110.82, 105.89, 61.05, 56.53, 55.67. HRMS (ESI) *m/z*: calcd for $C_{22}H_{22}N_4O_4$ ($M+H^+$) 407.1714 found 407.1717.

5.2.1.10. 2-Methoxy-5-(3-(3,4,5-trimethoxyphenyl)-[1,2,4]triazolo[4,3-a]pyridin-6-yl)phenol ***(7j)****.* Yield, 78%; mp: 183.2–183.7°C; ^{1}H NMR (400 MHz, $CDCl_3$) δ: 2.20 (s, 1H, OH), 3.96 (s, 6H, 2×CH_3O), 3.97 (s, 6H, 2×CH_3O), 6.97 (d, J = 8.4 Hz, 1H, Ph-H), 7.04 (s, 1H, Ph-H), 7.07 (s, 2H, Ph-H), 7.15 (s, 1H, Ph-H), 7.55 (d, J = 9.2 Hz, 1H, Pyridine-H), 7.87 (d, J = 9.6 Hz, 1H, Pyridine-H), 8.36 (s, 1H, Pyridine-H). ^{13}C NMR (100 MHz, $CDCl_3$) δ: 153.96, 149.80, 147.16, 146.92, 146.36, 139.78, 129.41, 128.54, 128.43, 121.81, 118.63, 118.61, 116.40, 113.11, 111.23, 105.78, 60.99, 56.45, 56.06. HRMS (ESI) *m/z*: calcd for $C_{22}H_{21}N_3O_5$ ($M+H^+$) 408.1554 found 408.1559.

5.2.1.11. 6-(4-Trifluoromethylphenyl)-3-(3,4,5-trimethoxyphenyl)-[1,2,4]triazolo[4,3-a]pyridine ***(7k)****.* Yield, 75%; mp: 199.3–199.5°C; ^{1}H NMR (400 MHz, $CDCl_3$) δ: 3.91 (s, 3H, CH_3O), 3.94 (s,6H, 2×CH_3O), 6.71 (s, 2H, Ph-H), 7.57 (d, J = 9.6 Hz, 1H, Pyridine-H), 7.88 (d, J = 8 Hz, 2H, Ph-H), 7.93 (d, J = 9.6 Hz, 1H, Pyridine-H), 8.04 (d, J = 8 Hz, 2H, Ph-H), 8.34 (s, 1H, Pyridine-H). ^{13}C NMR (100 MHz, $CDCl_3$) δ: 153.88, 150.19, 145.67, 138.85, 131.85 (d, J = 1.8 Hz, 2C), 130.24 (d, J = 1.1 Hz, 2C), 129.84, 129.00, 128.41, 126.37 (q, J_1 = 3.8 Hz, J_2 = 7.5 Hz, Hz, 1C), 123.31 (d, J = 204.8 Hz, 1C), 118.84, 116.69, 104.79, 60.94, 56.41. HRMS (ESI) *m/z*: calcd for $C_{22}H_{28}F_3N_3O_3$ ($M+H^+$) 430.1373 found 430.1365.

5.2.1.12. 4-(3-(3,4,5-trimethoxyphenyl)-[1,2,4]triazolo[4,3-a]pyridin-6-yl)phenol ***(7l)****.* Yield, 62%; mp: 212.5–213.1°C; ^{1}H NMR (400 MHz, DMSO-d_6) δ: 3.70 (s, 3H, CH_3O), 3.86 (s, 6H, 2×CH_3O), 6.99 (s, 2H, Ph-H), 7.01 (s, 2H, Ph-H), 7.76 (d, J = 9.6 Hz, 1H, Pyridine-H), 7.80 (d, J = 8.4 Hz, 2H, Ph-H), 7.91 (d, J = 9.6 Hz, 1H, Pyridine-H), 8.52 (s, 1H, Pyridine-H), 10.04 (s, 1H, OH). ^{13}C NMR (100 MHz, DMSO-d_6) δ: 159.40, 153.71, 149.45, 147.10, 138.06, 132.27, 130.18, 129.08, 127.91, 120.65, 117.59, 116.48, 115.85, 105.32, 60.48, 56.56. HRMS (ESI) *m/z*: calcd for $C_{21}H_{19}N_3O_4$ ($M+H^+$) 378.1449 found 378.1450.

*5.2.1.13. 6-Naphthalen-2-yl-3-(3,4,5-trimethoxyphenyl)-[1,2,4]triazolo[4,3-a]pyridine (**7m**).* Yield, 60%; mp: 185.6–185.9°C; ^{1}H NMR (400 MHz, $CDCl_3$) δ: 3.92 (s, 3H, CH_3O), 3.93 (s,6H, 2×CH_3O), 6.72 (s, 2H, Ph-H), 7.56 (dd, J_1 = 1.6 Hz, J_2 = 9.2 Hz, 1H, Pyridine-H), 7.61-7.64 (m, 2H, Naphthalene-H), 7.94 (dd, J_1 = 0.8 Hz, J_2 = 9.2 Hz, 1H, Pyridine-H), 7.97-7.99 (m, 3H, Naphthalene-H), 8.10 (d, J = 8.4 Hz, 1H, Naphthalene-H), 8.38 (s, 1H, Naphthalene-H), 8.45 (s, 1H, Pyridine-H). ^{13}C NMR (100 MHz, $CDCl_3$) δ: 153.84, 149.98, 147.11, 138.68, 133.81, 133.18, 132.14, 129.34, 129.28, 128.64, 128.41, 128.00, 127.93, 127.51, 127.10, 125.08, 123.95, 119.22, 116.63, 104.69, 60.95, 56.36. HRMS (ESI) *m/z*: calcd for $C_{25}H_{21}N_3O_3$ ($M+H^+$) 412.1656 found 412.1656.

*5.2.1.14. 6-(3-Methoxyphenyl)-3-(3,4,5-trimethoxyphenyl)-[1,2,4]triazolo[4,3-a]pyridine (**7n**).* Yield, 71%; mp: 127.2–127.6°C; ^{1}H NMR (400 MHz, $CDCl_3$) δ: 3.89 (s, 3H, CH_3O), 3.95 (s,6H, 2×CH_3O), 3.97 (s, 3H, CH_3O), 7.00 (d, J = 8.4 Hz, 1H, Ph-H), 7.06 (s, 3H, Ph-H), 7.12 (d, J = 7.2 Hz, 1H, Ph-H), 7.43 (t, J_1 = 7.6 Hz, J_2 = 15.6 Hz, 1H, Pyridine-H), 7.60 (d, J = 9.6 Hz, 1H, Pyridine-H), 7.93 (d, J = 9.6 Hz, 1H, Pyridine-H), 8.41 (s, 1H, Pyridine-H). ^{13}C NMR (100 MHz, $CDCl_3$) δ: 160.24, 154.01, 149.46, 146.90, 139.94, 137.44, 130.47, 129.01, 128.87, 121.41, 119.42, 119.26, 116.48, 113.55, 113.19, 105.84, 61.00, 56.47, 55.37. HRMS (ESI) *m/z*: calcd for $C_{22}H_{21}N_3O_4$ ($M+H^+$) 392.1606 found 392.1604

*5.2.1.15. 6-(5-Fluoro-2-methoxyphenyl)-3-(3,4,5-trimethoxyphenyl)-[1,2,4]triazolo[4,3-a]pyridine (**7o**).* Yield, 79%; mp: 193.2–194.°C; ^{1}H NMR (400 MHz, DMSO-d_6) δ: 3.77 (s, 3H, CH_3O), 3.80 (s,3H, CH_3O), 3.88 (s,6H, 2×CH_3O), 7.17 (dd, J_1 = 4.8 Hz, J_2 = 9.2 Hz, 1H, Ph-H), 7.20 (s, 2H, Ph-H), 7.23-7.28 (m, 1H, Ph-H), 7.42 (dd, J_1 = 3.2 Hz, J_2 = 9.2 Hz, 1H, Ph-H), 7.61 (dd, J_1 = 1.6 Hz, J_2 = 9.6 Hz, 1H, Pyridine-H), 7.88 (dd, J_1 = 0.8 Hz, J_2 = 9.6 Hz, 1H, Pyridine-H), 8.61 (m, J_1 = 1.2 Hz, J_2 = 2.4 Hz, 1H, Pyridine-H). ^{13}C NMR (100 MHz, DMSO-d_6) δ: 156.77 (d, J = 235.1 Hz, 1C), 153.85, 153.33 (d, J = 1.8 Hz, 1C), 149.41, 146.89, 139.32, 130.75, 126.63 (d, J = 8.1 Hz, 1C), 124.16 (d, J = 1.6 Hz, 1C), 123.27, 122.20, 117.57 (d, J = 24.1 Hz, 1C), 116.09 (d, J = 22.4 Hz, 1C), 114.82, 113.64 (d, J = 8.3 Hz, 1C), 106.41, 60.55, 56.73, 56.63. HRMS (ESI) *m/z*: calcd for $C_{22}H_{20}FN_3O_4$ ($M+H^+$) 410.1511 found 410.1505.

*5.2.1.16. 6-(2-Methoxyphenyl)-3-(3,4,5-trimethoxyphenyl)-[1,2,4]triazolo[4,3-a]Pyridine-H (**7p**).* Yield, 77%; mp: 180.5–180.9°C; ^{1}H NMR (400 MHz, DMSO-d_6) δ: 3.76 (s, 3H, CH_3O), 3.81 (s,3H, CH_3O), 3.87 (s,6H, 2×CH_3O), 7.06 (t, J_1 = 7.6 Hz, J_2 = 15.2 Hz, 1H, Ph-H), 7.17 (d, J = 8.4 Hz, 1H, Ph-H), 7.20 (s, 2H, Ph-H), 7.43 (t, J_1 = 7.6 Hz, J_2 = 15.2 Hz, 1H, Ph-H), 7.49 (d, J= 7.2 Hz, 1H, Ph-H), 7.60 (d, J= 9.6 Hz, 1H, Pyridine-H), 7.87 (d, J= 9.6 Hz, 1H, Pyridine-H), 8.53 (s, 1H, Pyridine-H). ^{13}C NMR (100 MHz, DMSO-d_6) δ: 156.87, 153.84, 149.42, 146.75, 139.21, 131.10, 130.88, 130.38, 125.25, 125.23, 122.58, 122.29, 121.41, 114.77, 112.29, 106.31, 60.55, 56.60, 56.10. HRMS (ESI) *m/z*: calcd for $C_{22}H_{21}N_3O_4$ ($M+H^+$) 392.1605 found 392.1602.

*5.2.1.17. 6-(4-Fluoro-2-methoxyphenyl)-3-(3,4,5-trimethoxyphenyl)-[1,2,4]triazolo[4,3-a]pyridine (**7q**).* Yield, 75%; mp: 203.1–204.8°C; ^{1}H NMR (400 MHz, DMSO-d_6) δ: 3.76 (s, 3H, CH_3O), 3.83 (s, 3H, CH_3O), 3.87 (s, 6H, 2×CH_3O), 6.90 (t, J_1 = 8.4 Hz, J_2 = 16.8 Hz, 1H, Ph-H), 7.09 (d, J = 11.6 Hz, 1H, Pyridine-H), 7.19 (s, 2H, Ph-H), 7.51 (d, J = 8 Hz, 1H, Ph-H), 7.56 (d, J = 10.4 Hz, 1H, Pyridine-H), 7.87 (d, J = 9.6 Hz, 1H, Ph-H), 8.51 (s, 1H, Pyridine-H). ^{13}C NMR (100 MHz, DMSO-d_6) δ: 163.56 (d, J = 243.4 Hz, 1C), 158.32 (d, J = 10.2 Hz, 1C), 153.83, 149.40, 146.76, 139.21, 132.11(d, J = 10.1 Hz, 1C), 131.04, 124.48, 122.70, 122.25, 121.71 (d, J = 3.2 Hz, 1C), 114.80, 107.63 (d, J = 20.9 Hz, 1C), 106.30, 100.60 (d, J = 25.8 Hz, 1C), 60.54, 56.60. HRMS (ESI) *m/z*: calcd for $C_{22}H_{20}FN_3O_4$ ($M+H^+$) 410.1511 found 410.1506.

*5.2.1.18. 6-(2-Trifluoromethoxyphenyl)-3-(3,4,5-trimethoxyphenyl)-[1,2,4]triazolo[4,3-a]pyridine (**7r**).* Yield, 82 %; mp: 187.2–187.9°C; ^{1}H NMR (400 MHz, DMSO-d_6) δ: 3.76 (s, 3H, CH_3O), 3.87 (s, 6H, 2×CH_3O), 7.19 (s, 2H, Ph-H), 7.55-7.62 (m, 4H, Ph-H), 7.75 (d, J= 6.4 Hz, 1H, Pyridine-H), 7.97 (d, J= 9.6 Hz, 1H, Pyridine-H), 8.65 (s, 1H, Pyridine-H). ^{13}C NMR (150 MHz, $CDCl_3$) δ: 154.02, 149.68, 147.11, 146.30 (d, J = 1.31 Hz, 1C), 139.88, 131.16, 130.25, 130.16, 130.16, 129.43, 127.75, 123.91, 122.08, 121.84, 121.62, 120.32 (q, J_1 = 257.34 Hz, J_2 = 514.68 Hz, 1C), 116.43, 105.73, 61.00, 56.38. HRMS (ESI) *m/z*: calcd for $C_{22}H_{18}F_3N_3O_4$ ($M+H^+$) 446.1322 found 446.1316.

*5.2.1.19. 6-(2,4-Dimethoxyphenyl)-3-(3,4,5-trimethoxyphenyl)-[1,2,4]triazolo[4,3-a]pyridine (**7s**).* Yield, 79%; mp: 105.9–106.5°C; ^{1}H NMR (400 MHz, DMSO-d_6) δ: 3.70 (s, 3H, CH_3O), 3.87 (s, 6H, 2×CH_3O), 3.89 (s, 3H, CH_3O), 3.91 (s, 3H, CH_3O), 6.78 (d, J= 8.4 Hz, 1H, Ph-H), 6.84 (s, 1H, Ph-H), 6.93 (s, 2H, Ph-H), 7.56 (d, J = 8.4 Hz, 1H, Ph-H), 7.79 (d, J = 9.2 Hz, 1H, Pyridine-H), 7.91 (d, J = 9.6 Hz, 1H, Pyridine-H), 8.16 (s, 1H, Pyridine-H). ^{13}C NMR (100 MHz, DMSO-d_6) δ: 163.08, 158.65, 153.67, 149.31, 145.69, 137.99, 133.23, 132.03, 128.85, 127.18, 121.95, 115.59, 107.96, 106.50, 105.03, 99.45, 60.46, 56.40, 55.99, 55.96. HRMS (ESI) *m/z*: calcd for $C_{23}H_{23}N_3O_5$ ($M+H^+$) 422.1711 found 422.1707.

*5.2.1.20. 5-Methoxy-2-[3-(3,4,5-trimethoxyphenyl)-[1,2,4]triazolo[4,3-a]pyridin-6-yl]-phenol (**7t**).* Yield, 70%; mp: 195.2–195.8°C; ^{1}H NMR (400 MHz, $CDCl_3$) δ: 3.51 (s, 1H, OH), 3.91 (s, 3H, CH_3O), 3.93 (s, 6H, 2×CH_3O), 4.01 (s, 3H, CH_3O), 6.71 (s, 2H, Ph-H), 7.06 (d, J = 8.4 Hz, 1H, Ph-H), 7.37 (dd, J_1 = 2 Hz, J_2 = 8.4 Hz, 1H, Ph-H), 7.51 (dd, J_1 = 1.6 Hz, J_2 = 9.6 Hz, 1H, Pyridine-H), 7.69 (d, J = 2 Hz, 1H, Ph-H), 7.86 (d, J = 9.6 Hz, 1H, Pyridine-H), 8.37 (s, 1H, Pyridine-H). ^{13}C NMR (100 MHz, $CDCl_3$) δ: 162.21, 158.61, 153.88, 148.79, 145.31, 138.79, 132.03, 129.57, 129.14, 125.78, 120.08, 116.61, 107.01, 104.80, 104.33, 102.49, 60.96, 56.41, 55.41. HRMS (ESI) *m/z*: calcd for $C_{22}H_{21}N_3O_5$ ($M+H^+$) 408.1554 found 408.1556.

*5.2.1.22. 6-(2-Methoxypyridin-3-yl)-3-(3,4,5-trimethoxyphenyl)-[1,2,4]triazolo[4,3-a]pyridine (**7u**).* Yield, 68 %; mp: 203.5–204.0°C; ^{1}H NMR (400 MHz, DMSO-d_6) δ: 3.76 (s, 3H, CH_3O), 3.88

(s,6H, 2×CH_3O), 3.92 (s, 3H, CH_3O), 7.13 (dd, J_1 = 4.8 Hz, J_2 = 6.4 Hz, 1H, Pyridine-H), 7.21 (s, 2H, Ph-H), 7.67 (d, *J*= 9.6 Hz, 1H, Pyridine-H), 7.90 (d, *J*= 9.6 Hz, 1H, Pyridine-H) 7.96 ((d, *J*= 6.8 Hz, 1H, Pyridine-H), 8.24 (d, *J*= 4.8 Hz, 1H, Pyridine-H), 8.69 (s, 1H, Pyridine-H). ^{13}C NMR (100 MHz, DMSO-d_6) δ: 160.75, 153.84, 149.44, 147.10, 146.89, 139.64, 139.25, 130.28, 123.52, 123.27, 122.17, 119.65, 118.03, 115.06, 106.32, 60.54, 56.61, 53.95. HRMS (ESI) *m/z*: calcd for $C_{21}H_{20}N_4O_4$ ($M+H^+$) 393.1558 found 393.1557.

5.2.2 General procedure for the preparation of derivatives ***8a–h***.

(E)-5-bromo-2-(2-(substituted benzylidene)hydrazinyl)pyridine ***12a–h***.

A solution of 5-bromo-2-hydrazinylpyridine **8** (2.2 g, 10mmol) in ethanol (80 mL) was added to appropriate benzaldehydes (10 mmol) and the resulting mixture was stirred for about 3-5 h at room temperature. The crude product was filtered, washed with ethanol (10 mL× 3) and dried to give compounds **12a–h** in the yield of 73-89%, which was used for next step reaction without purification.

6-Bromo-3-substituted -[1,2,4]triazolo[4,3-a]pyridine ***13a–h***.

To the solution of **12a–h** (0.25mmol) in CH_2Cl_2 (100 mL) was added iodobenzene diacetate (1.0mmol) at room temperature under nitrogen atmosphere. The resulting mixture was stirred for 8-10 h. After completion of the reaction, the mixture was poured into water and extracted with dichloromethane. The organic extract was washed with brine, dried, and evaporated to provide a crude solid, which was washed with methanol (3 mL ×2) and dried to afford **13a–h** in yields of 70-83%.

*6-Bromo-3-p-tolyl-[1,2,4]triazolo[4,3-a]pyridine (**13a**).* Yield, 81%; mp: 185.3–187.2°C; ^{1}H NMR (400 MHz, DMSO-d_6) δ: 2.44 (s, 3H, CH_3), 7.35 (d, *J* = 7.6 Hz, 2H, Ph-H), 7.83 (d, *J* = 9.6 Hz, 1H, Pyridine-H), 7.86 (d, *J* = 7.6 Hz, 2H, Ph-H), 7.97 (d, *J* = 9.6 Hz, 1H, Pyridine-H), 8.59 (s, 1H, Pyridine-H). ^{13}C NMR (150 MHz, $CDCl_3$) δ: 148.98, 146.84, 140.92, 130.66, 130.18, 128.18, 123.12, 122.65, 117.44, 109.33, 21.55.

*6-Bromo-3-(4-methoxy-phenyl)-[1,2,4]triazolo[4,3-a]pyridine (**13b**).* Yield, 79%; mp: 204.9.3–206.8°C; ^{1}H NMR (400 MHz, $CDCl_3$) δ: 3.91 (s, 3H, CH_3O), 3.92 (s, 3H, CH_3O), 7.11 (d, *J* = 8.4 Hz, 2H, Ph-H), 7.49 (d, *J* = 9.2 Hz, 1H, Pyridine-H), 7.80 (d, *J* = 8.4 Hz, 2H, Ph-H), 7.88 (d, *J* = 9.6 Hz, 1H, Pyridine-H), 8.32 (s, 1H, Pyridine-H). ^{13}C NMR (150 MHz, $CDCl_3$) δ: 161.43, 148.65, 146.62, 131.00, 129.85, 122.62, 117.97, 117.32, 114.99, 109.52, 55.52.

*6-Bromo-3-(4-methoxy-3-nitro-phenyl)-[1,2,4]triazolo[4,3-a]pyridine (**13c**).* Yield, 76%; mp:

215.5–217.4°C; ^{1}H NMR (400 MHz, DMSO-d_6) δ: 4.05 (s, 3H, CH_3O), 7.60 (d, J = 8.8 Hz, 1H, Ph-H), 7.90 (d, J = 9.6 Hz, 1H, Pyridine-H), 7.99 (d, J = 9.6 Hz, 1H, Pyridine-H), 8.31 (dd, J_1 = 2.4 Hz, J_2 = 8.8 Hz, 1H, Ph-H), 8.55 (d, J = 2 Hz, 1H, Ph-H), 8.69 (s, 1H, Pyridine-H). ^{13}C NMR (150 MHz, $CDCl_3$) δ: 154.39, 149.25, 144.42, 139.94, 134.17, 131.22, 125.13, 122.04, 118.50, 117.65, 114.81, 110.29, 56.95.

6-Bromo-3-(4-chloro-phenyl)-[1,2,4]triazolo[4,3-a]pyridine ***(13d)***. Yield, 83%; mp: 170.1–172.3°C; ^{1}H NMR (400 MHz, $CDCl_3$) δ: 7.55 (d, J = 9.2 Hz, 1H, Pyridine-H), 7.58 (d, J = 8 Hz, 2H, Ph-H), 7.84 (d, J = 8 Hz, 2H, Ph-H), 7.93 (d, J = 9.6 Hz, 1H, Pyridine-H), 8.34 (s, 1H, Pyridine-H). ^{13}C NMR (150 MHz, $CDCl_3$) δ: 150.72, 148.14, 132.61, 132.44, 131.21, 128.64, 128.17, 123.87, 107.83, 105.15.

6-Bromo-3-(3,4-dichloro-phenyl)-[1,2,4]triazolo[4,3-a]pyridine ***(13e)***. Yield, 80%; mp: 182.6–184.4°C; ^{1}H NMR (400 MHz, DMSO-d_6) δ: 7.91 (d, J = 9.6 Hz, 1H, Pyridine-H), 7.84 (d, J = 8.4 Hz, 1H, Ph-H), 7.99 (d, J = 9.6 Hz, 1H, Pyridine-H), 8.22 (d, J = 8.8 Hz, 1H, Ph-H), 8.38 (s, 1H, Ph-H), 8.69 (s, 1H, Pyridine-H). ^{13}C NMR (150 MHz, $CDCl_3$) δ: 149.31, 144.59, 135.10, 134.09, 131.58, 131.23, 130.00, 127.08, 125.96, 122.22, 117.60, 110.23.

5-(6-Bromo-[1,2,4]triazolo[4,3-a]pyridin-3-yl)-2-methoxy-phenol ***(13f)***. Yield, 77%; mp: 235.5–237.4°C; ^{1}H NMR (400 MHz, DMSO-d_6) δ: 3.71 (s, 3H, CH_3O), 7.17 (d, J = 8.4 Hz, 1H, Ph-H), 7.39 (s, 1H, Ph-H), 7.40 (d, J = 8.4 Hz, 1H, Ph-H), 7.86 (d, J = 9.6 Hz, 1H, Pyridine-H), 7.93 (d, J = 9.6 Hz, 1H, Pyridine-H), 8.59 (s, 1H, Pyridine-H), 9.50 (s, 1H, OH). ^{13}C NMR (150 MHz, $CDCl_3$) δ: 148.84, 148.68, 146.56, 130.81, 122.75, 120.66, 118.82, 117.30, 114.50, 111.42, 109.37, 56.13.

6-Bromo-3-(4-fluoro-phenyl)-[1,2,4]triazolo[4,3-a]pyridine ***(13g)***. Yield, 79%; mp: 161.5–163.2°C; ^{1}H NMR (400 MHz, DMSO-d_6) δ: 7.46 (t, J = 8.8 Hz, 2H, Ph-H), 7.83 (d, J = 9.6 Hz, 1H, Pyridine-H), 7.96 (d, J = 9.6 Hz, 1H, Pyridine-H), 7.92 (dd, J_1 = 5.6 Hz, J_2 = 8.4 Hz, 2H, Ph-H), 8.66 (s, 1H, Pyridine-H). ^{13}C NMR (150 MHz, $CDCl_3$) δ: 160.53 (d, J = 284.5 Hz), 155.43, 149.95, 133.51, 132.49 (d, J = 10.5 Hz), 129.05 (d, J = 2.7 Hz), 125.95, 117.43 (d, J = 24.3 Hz), 109.65, 103.26.

5-(6-Bromo-[1,2,4]triazolo[4,3-a]pyridin-3-yl)-2-methoxy-phenylamine ***(13h)***. Yield, 70%; mp: 202.7–204.9°C; ^{1}H NMR (400 MHz, DMSO-d_6) δ: 3.96 (s, 3H, CH_3O), 6.22 (s, 2H, NH_2), 6.98 (d, J = 8.4 Hz, 1H, Ph-H), 7.28 (d, J = 8.4 Hz, 1H, Ph-H), 7.22 (s, 1H, Ph-H), 7.51 (d, J = 9.6 Hz, 1H, Pyridine-H), 7.89 (d, J = 9.2 Hz, 1H, Pyridine-H), 8.46 (s, 1H, Pyridine-H). ^{13}C NMR (150 MHz, $CDCl_3$) δ: 150.97, 149.88, 145.46, 138.24, 137.53, 134.57, 123.95, 119.51, 115.44, 110.01, 108.65, 100.24, 55.86.

*General procedure for the preparation of the **8a**–**h**.*

To the solution of **13** (0.40 mmol), $Pd_2(dba)_3$ (0.04 mmol), xantphos (0.05 mmol), K_3PO_4 (0.48 mmol) and (3,4,5-trimethoxyphenyl)boronic acid (0.41 mmol) in DMF/H_2O (20 mL, 5:1) was degassed and purged with N_2 for about three times. After stirred at 80°C for about 8-12 h (indicated by TLC) under N_2 atmosphere, the reaction mixture was poured into H_2O (50 mL) and extracted with ethyl acetate (80 mL×3). The combined organics were washed with brine (10 mL×3), dried over anhydrous Na_2SO_4, filtered and concentrated under vacuum to give a residue, which was purified by column chromatography using a mixture of petroleum ether and acetone (3:1) as an eluent to give the target compounds **8a**–**h** in yields of 59–84%.

*5.2.2.1. 3-p-Tolyl-6-(3,4,5-trimethoxyphenyl)-[1,2,4]triazolo[4,3-a]pyridine (**8a**).* Yield, 84%; mp: 182.1–182.9°C; ^{1}H NMR (400 MHz, DMSO-d_6) δ: 2.44 (s, 3H, CH_3), 3.71 (s, 3H, CH_3O), 3.87 (s,6H, 2×CH_3O), 7.00 (s, 2H, Ph-H), 7.45 (d, *J* = 7.6 Hz, 2H, Ph-H), 7.79 (d, *J* = 9.6 Hz, 1H, Pyridine-H), 7.89 (d, *J* = 7.6 Hz, 2H, Ph-H), 7.94 (d, *J* = 9.6 Hz, 1H, Pyridine-H), 8.58 (s, 1H, Pyridine-H). ^{13}C NMR (100 MHz, $CDCl_3$) δ: 153.80, 149.76, 148.00, 140.55, 138.65, 132.18, 130.05, 129.03, 128.50, 128.13, 123.66, 119.26, 116.47, 104.70, 60.94, 56.39, 21.46. HRMS (ESI) *m/z*: calcd for $C_{22}H_{21}N_3O_3$ ($M+H^+$) 376.1656 found 376.1683.

*5.2.2.2. 3-(4-Methoxyphenyl)-6-(3,4,5-trimethoxyphenyl)-[1,2,4]triazolo[4,3-a]pyridine (**8b**).* Yield, 80%; mp: 205.7–206.1°C; ^{1}H NMR (400 MHz, $CDCl_3$) δ: 3.91 (s, 3H, CH_3O), 3.92 (s, 3H, CH_3O), 3.93 (s,6H, 2×CH_3O), 6.70 (s, 2H, Ph-H), 7.13 (d, *J* = 8.4 Hz, 2H, Ph-H), 7.50 (d, *J* = 9.2 Hz, 1H, Pyridine-H), 7.80 (d, *J* = 8.4 Hz, 2H, Ph-H), 7.87 (d, *J* = 9.6 Hz, 1H, Pyridine-H), 8.29 (s, 1H, Pyridine-H). ^{13}C NMR (100 MHz, $CDCl_3$) δ: 161.07, 153.80, 149.69, 146.93, 138.65, 132.23, 129.74, 128.94, 128.35, 119.18, 118.84, 116.49, 114.81, 104.71, 60.94, 56.39, 55.42. HRMS (ESI) *m/z*: calcd for$C_{22}H_{21}N_3O_4$ ($M+H^+$) 392.1610 found 392.1586.

*5.2.2.3. 3-(4-Methoxy-3-nitrophenyl)-6-(3,4,5-trimethoxyphenyl)-[1,2,4]triazolo[4,3-a]pyridine (**8c**).* Yield, 78%; mp: 202.8–203.0°C; ^{1}H NMR (400 MHz, DMSO-d_6) δ: 3.71 (s, 3H, CH_3O), 3.87 (s, 6H, 2×CH_3O), 4.05 (s,3H, CH_3O), 7.02 (s, 2H, Ph-H), 7.61 (d, *J* = 8.8 Hz, 1H, Ph-H), 7.87 (d, *J* = 9.6 Hz, 1H, Pyridine-H), 7.96 (d, *J* = 9.6 Hz, 1H, Pyridine-H), 8.28 (dd, J_1 = 2.4 Hz, J_2 = 8.8 Hz, 1H, Ph-H), 8.52 (d, *J* = 2 Hz, 1H, Ph-H), 8.66 (s, 1H, Pyridine-H). ^{13}C NMR (100 MHz, $CDCl_3$) δ: 154.23, 153.92, 149.99, 144.63, 138.85, 134.46, 131.58, 129.91, 128.87, 128.34, 124.78, 118.97, 118.63, 116.67, 114.87, 104.55, 60.96, 56.87, 56.35. HRMS (ESI) *m/z*: calcd for $C_{22}H_{20}N_4O_6$ ($M+H^+$) 437.1455 found 437.1445.

*5.2.2.4. 3-(4-Chlorophenyl)-6-(3,4,5-trimethoxyphenyl)-[1,2,4]triazolo[4,3-a]pyridine (**8d**).* Yield, 77%; mp: 230.1–232.5°C; ^{1}H NMR (400 MHz, $CDCl_3$) δ: 3.91 (s, 3H, CH_3O), 3.94 (s, 6H,

2×CH_3O), 6.70 (s, 2H, Ph-H), 7.53 (d, *J* = 9.2 Hz, 1H, Pyridine-H), 7.59 (d, *J* = 8 Hz, 2H, Ph-H), 7.82 (d, *J* = 8 Hz, 2H, Ph-H), 7.89 (d, *J* = 9.6 Hz, 1H, Pyridine-H), 8.28 (s, 1H, Pyridine-H). ^{13}C NMR (100 MHz, $CDCl_3$) δ: 153.85, 149.98, 146.00, 138.79, 136.40, 131.96, 129.70, 129.45, 128.71, 125.13, 118.92, 116.60, 104.75, 60.94, 56.41. HRMS (ESI) *m/z*: calcd for $C_{21}H_{18}ClN_3O_3$ ($M+H^+$) 396.1115 found 396.1097.

5.2.2.5. 3-(3,4-Dichlorophenyl)-6-(3,4,5-trimethoxyphenyl)-[1,2,4]triazolo[4,3-a]pyridine ***(8e)****.* Yield, 81%; mp:140.2–140.5°C; ^{1}H NMR (400 MHz, DMSO-d_6) δ: 3.71 (s, 3H, CH_3O), 3.87 (s, 6H, 2×CH_3O), 7.03 (s, 2H, Ph-H), 7.85 (d, *J* = 9.6 Hz, 1H, Pyridine-H), 7.89 (d, *J* = 8.4 Hz, 1H, Ph-H), 7.98 (d, *J* = 9.6 Hz, 1H, Pyridine-H), 8.02 (d, *J* = 8.8 Hz, 1H, Ph-H), 8.28 (s, 1H, Ph-H), 8.67 (s, 1H, Pyridine-H). ^{13}C NMR (100 MHz, $CDCl_3$) δ: 153.88, 150.10, 144.87, 138.84, 134.66, 133.88, 131.76, 131.45, 129.93, 129.85, 128.95, 127.07, 126.53, 118.75, 116.66, 104.71, 60.96, 56.38. HRMS (ESI) *m/z*: calcd for $C_{21}H_{17}Cl_2N_3O_3$ ($M+H^+$) 430.0725 found 430.0710.

5.2.2.6. 2-methoxy-5-(6-(3,4,5-trimethoxyphenyl)-[1,2,4]triazolo[4,3-a]pyridin-3-yl)phenol ***(8f)****.* Yield, 59%; mp: 253.0–253.7°C; ^{1}H NMR (400 MHz, DMSO-d_6) δ: 3.71 (s, 3H, CH_3O), 3.87 (s, 6H, 2×CH_3O), 6.99 (s, 2H, Ph-H), 7.15 (d, *J* = 8.4 Hz, 1H, Ph-H), 7.37 (s, 1H, Ph-H), 7.42 (d, *J* = 8.4 Hz, 1H, Ph-H), 7.76 (d, *J* = 9.6 Hz, 1H, Pyridine-H), 7.91 (d, *J* = 9.6 Hz, 1H, Pyridine-H), 8.55 (s, 1H, Pyridine-H), 9.50 (s, 1H, OH). ^{13}C NMR (100 MHz, DMSO-d_6) δ: 153.76, 149.64, 149.53, 147.49, 146.84, 138.16, 132.28, 129.13, 127.97, 120.68, 119.69, 119.42, 115.88, 115.49, 113.04, 105.37, 60.49, 56.61, 56.08. HRMS (ESI) *m/z*: calcd for $C_{22}H_{21}N_3O_5$ ($M+H^+$) 409.1559 found 409.1588.

5.2.2.7. 3-(4-Fluorophenyl)-6-(3,4,5-trimethoxyphenyl)-[1,2,4]triazolo[4,3-a]pyridine ***(8g)****.* Yield, 75%; mp: 175.5–177.4°C; ^{1}H NMR (400 MHz, DMSO-d_6) δ: 3.71 (s, 3H, CH_3O), 3.87 (s, 3H, 2×CH_3O), 7.01 (s, 2H, Ph-H), 7.47 (t, J_1 = 8.8 Hz, J_2 = 17.6 Hz, 2H, Ph-H), 7.81 (d, *J* = 9.6 Hz, 1H, Pyridine-H), 7.95 (d, *J* = 9.6 Hz, 1H, Pyridine-H), 7.89 (dd, J_1 = 5.6 Hz, J_2 = 8.4 Hz, 2H, Ph-H), 8.59 (s, 1H, Pyridine-H). ^{13}C NMR (100 MHz, DMSO-d_6) δ: 163.38 (d, *J* = 246.2 Hz, 1C), 153.74, 149.77, 146.13, 138.23, 132.11, 131.14, 131.09 (d, *J* = 8.7 Hz, 2C), 129.44, 128.18, 123.61 (d, *J* = 3.1 Hz, 1C), 120.78, 116.77 (d, *J* = 21.7 Hz, 2C), 115.81, 105.48, 60.49, 56.62. HRMS (ESI) *m/z*: calcd for $C_{21}H_{18}FN_3O_3$ ($M+H^+$) 380.1410 found 380.1397.

5.2.2.8. 2-Methoxy-5-[6-(3,4,5-trimethoxyphenyl)-[1,2,4]triazolo[4,3-a]pyridin-3-yl]-phenylamine ***(8h)****.* Yield, 70%; mp: 188.2–190.9°C; ^{1}H NMR (400 MHz, $CDCl_3$) δ: 3.91 (s, 3H, CH_3O), 3.94 (s, 6H, 2×CH_3O), 3.96 (s, 3H, CH_3O), 4.06 (s,2H, NH_2), 6.70 (s, 2H, Ph-H), 6.97 (d, *J* = 8.4 Hz, 1H, Ph-H), 7.18 (d, *J* = 8.4 Hz, 1H, Ph-H), 7.22 (s, 1H, Ph-H), 7.48 (d, *J* = 9.6 Hz, 1H, Pyridine-H), 7.85 (d, *J* = 9.2 Hz, 1H, Pyridine-H), 8.34 (s, 1H, Pyridine-H). ^{13}C NMR (100 MHz, $CDCl_3$) δ: 153.77, 149.63, 148.66, 147.32, 138.56, 137.24, 132.35, 128.71, 128.27, 119.53, 119.16, 118.11, 116.38, 114.45, 110.49, 104.71, 60.94, 56.39, 55.59. HRMS (ESI) *m/z*: calcd for $C_{22}H_{22}N_4O_4$

($M+H^+$) 407.1719 found 407.1704.

595 *5.3 Biological evaluation*

5.3.1 Antiproliferative activity

The antitumor activities of tested samples were measured against human epithelial cervical cancer (HeLa) cell lines by the typical MTT assay *in vitro*. The cancer cell lines were cultured in RPMI-1640 medium supplemented with 10% fetal bovine serum (FBS) in a humidified 5% CO_2 600 atmosphere at 37 °C. All of tested samples were prepared by dissolving in dimethyl sulfoxide (DMSO) at 50 mM concentration and diluted with the medium into a series of concentrations. Exponentially growing cells were plated in 96-well plates (2×10^3 cells/well) and incubated for attachment at 37 °C for 24 h. The culture medium was then changed, and cells grew in medium with the tested compounds. DMSO (0.1%) and CA-4 were used as negative and positive control, 605 respectively. Cells were incubated at 37 °C for 48 h. After the treatment period, 20 μL of MTT solution (5 mg/mL) was added to each well, and the plates were incubated for 4 h at 37°C. The medium was then aspirated and formazan crystals were dissolved in DMSO (200μL) for about 10 mins. The absorbance at 570 nm (Abs) of the suspension was measured by a microplate reader (Bio-Rad laboratories, USA). Percentage of relative viability was calculated using the following 610 equation: % inhibition = $(Abs_{control} - Abs_{compound})/Abs_{control}\times100\%$. The IC_{50} values of the tested samples were measured by treating cells with drugs of various concentrations and analyzed by use of the prism statistical package.

5.3.2 Cell cycle analysis

Flow cytometric analysis was performed to investigate the effect of **7i** on cell cycle phase 615 distribution of human cervical cancer cell lines (HeLa). The cells were plated in 6-well plate and incubated overnight at 37 °C. After grew to about 70% confluence in 60 mm dish, cells were incubated with different concentrations (12, 24, and 48 nM) or vehicle for 24 h. Control and treated cells were harvested, washed with PBS, and fixed in 75% ice-cold ethanol at 4 °C overnight. Subsequently, the cells were washed with PBS, incubated with 50 μg/mL of RNase at 37 °C for 30 620 min, and stained with 50 μg/mL of propidium iodide, and finally subjected to flow cytometry (Beckman Coulter).

5.3.3 Apoptosis analysis

HeLa cells were seed into 6-well plates (2×10^5 cells/well), incubated with compound **7i** at indicated concentrations or vehicle for 24h. Cells were harvested and incubated with 5 μL of Annexin-V/FITC in binding buffer (10 mM HEPES, 140 mM NaCl, and 2.5 mM $CaCl_2$ at pH 7.4) and PI solution (10 μL) for 15 min. PI solution (10 μL) was then added to the medium for another 10 min incubation. Almost 10000 events were collected for each sample and analyzed with flow cytometry. Finally, the percentag of apoptotic cells was examined using FlowJo 7.6 software.

5.3.4 Immunocytochemistry

Confocal microscopy was performed to explore the effects of the most potent compound **7i** on HeLa cytoskeleton. HeLa cells (9×10^3 cells/well) were plated on glass coverslips in 24-well plates and allowed to attach overnight. After treatment with 1-fold IC_{50} concentration of **7i**, CA-4 or 0.1% DMSO (control) for 6 h, cells were rinsed twice with PBS, fixed with 4% paraformaldehyde, and then permeabilized with 0.1% Triton X-100. After blocking with 5% BSA for 60 min, the coverslips were incubated at 4°C overnight with primary antibodies (α-tubulin mouse monoclonal antibody and β-tubulin rabbit monoclonal antibody). After washing, the cells were incubated with the following secondary antibodies: Alexa Fluor® 555 conjugate anti-rabbit IgG and FITC AffiniPure goat anti-mouse IgG. Nuclei were visualized with DAPI, and then, images were obtained by a laser scanning confocal microscope (Carl Zeiss LSM 880).

5.3.5 In vitro tubulin polymerization assay

The tubulin polymerization activity assay *in vitro* was carried out according to our previously reported method [16].

5.3.6 Molecular modeling

Molecular modelling studies were carried out with the SURFLEX module of SYBYL 7.3 package [30], and the crystal strucure of tubulin complexed with Combretastatin A-4 (PDB: 5lyj) was down loaded from the PDB data bank (http://www.rcsb.org/pdb) [31]. Structural energy minimization process was performed using the Tripos force field with a distance–dependent dielectric and powell gradient algorithm with a convergence criterion of 0.005 kcal/mol Å. Additionally, partial atomic charges were calculated using Gasteiger–Hückel method and all the other parameters were assigned default values in the docking process. Finally, the best 20 ranked conformations with different scores were obtained and the best ranking pose was visualized with PyMOL [32].

Acknowledgments

This present work was financially supported by the Natural Science Foundation of Guangdong Province, China (Grant No. 2018B030311067), and the Science and Technology Program of Guangzhou City, China (Grant No. 201707010198).

Appendix A. Supplementary data

Supplementary data related to this article can be found at http://dx.doi.org/10.1016/j.ejmech.2020.xx.xxx.

References

[1] M.A. Jordan, L. Wilson. Microtubules as a target for anticancer drugs. Nat. Rev. Cancer, 4 (2004) 253−265.

[2] H.Y. Kueh, T.J. Mitchison. Structural plasticity in actin and tubulin polymer dynamics. Science, 325 (2009) 960−963.

[3] C. Dumontet, M.A. Jordan. Microtubule-binding agents: a dynamic field of cancer therapeutics. Nat. Rev. Drug Discov. 9 (2010) 790−803.

[4] F. Naaz, M.R. Haider, S. Shafi, M.S. Yar. Anti-tubulin agents of natural origin: targeting taxol, vinca, and colchicine binding domains. Eur. J. Med. Chem. 171 (2019) 310−331.

[5] W. Li, H. Sun, S. Xu, Z. Zhu, J. Xu. Tubulin inhibitors targeting the colchicine binding site: a perspective of privileged structures. Future Med. Chem. 9 (2017) 1765−1794.

[6] W. Li, F. Xu, W. Shuai, H. Sun, H. Yao, C. Ma, S. Xu, H. Yao, Z. Zhu, D.H. Yang, Z.S. Chen, J. Xu. Discovery of novel quinoline-chalcone derivatives as potent antitumor agents with microtubule polymerization inhibitory activity. J. Med. Chem. 62 (2019) 993−1013.

[7] E.A. Perez. Microtubule inhibitors: differentiating tubulin-inhibiting agents based on mechanisms of action, clinical activity, and resistance. Mol. Cancer Ther. 8 (2009) 2086−2095.

[8] M.J. Hu, B. Zhang, H.K. Yang, Y. Liu, Y.R. Chen, T.Z. Ma, L. Lu, W.W. You, P.L. Zhao, Design, synthesis and molecular docking studies of novel indole-pyrimidine hybrids as tubulin polymerization inhibitors. Chem. Biol. Drug Des. 86 (2015) 1491−1500.

[9] Y.L. Zhang, B.Y. Li, R. Yang, L.Y. Xia, A.L. Fan, Y.C. Chu, L.J. Wang, Z.C. Wang, A.Q. Jiang, H.L. Zhu. A class of novel tubulin polymerization inhibitors exert effective anti-tumor activity via mitotic catastrophe. Eur. J. Med. Chem. 163 (2019) 896−910.

[10] P.C. Diao, Q. Li, M.J. Hu, Y.F. Ma, W.W. You, K.H. Hong, P.L. Zhao. Synthesis and biological evaluation of novel indole-pyrimidine hybrids bearing morpholine and thiomorpholine moieties. Eur. J. Med. Chem. 134 (2017) 110−118.

[11] S. Banerjee, K.E. Arnst, Y. Wang, G. Kumar, S. Deng, L. Yang, G.B. Li, J. Yang, S.W. White, W. Li, D.D. Miller. Heterocyclic-fused pyrimidines as novel tubulin polymerization inhibitors targeting the colchicine binding site: structural basis and antitumor efficacy. J. Med. Chem. 61

(2018) 1704−1718.

[12] A. Siddiqui-Jain, J.P. Hoj, D.W. Cescon, M.D. Hansen. Pharmacology and in vivo efficacy of pyridine-pyrimidine amides that inhibit microtubule polymerization. Bioorg. Med. Chem. Lett. 28 (2018) 934–941.

[13] P.L. Zhao, W.F. Ma, A.N. Duan, M. Zou, Y.C. Yan, W.W. You, S.G. Wu, One-pot synthesis of novel isoindoline-1,3-dione derivatives bearing 1,2,4-triazole moiety and their preliminary biological evaluation. Eur. J. Med. Chem. 54 (2012) 813−822.

[14] F. Yang, C.P. He, P.C. Diao, K.H. Hong, J.J. Rao, P.L. Zhao. Discovery and optimization of 3,4,5-trimethoxyphenyl substituted triazolylthioacetamides as potent tubulin polymerization inhibitors. Bioorg. Med. Chem. Lett. 29 (2019) 22−27.

[15] M. Mustafa, S. Anwar, F. Elgamal, E.R. Ahmed, O.M. Aly. Potent combretastatin A-4 analogs containing 1,2,4-triazole: synthesis, antiproliferative, anti-tubulin activity, and docking study. Eur. J. Med. Chem. 183 (2019) 111697. doi: 10.1016/j.ejmech.

[16] Y.H. Li, B. Zhang, H.K. Yang, Q. Li, P.C. Diao, W.W. You, P.L. Zhao. Design, synthesis, and biological evaluation of novel alkylsulfanyl-1,2,4-triazoles as cis-restricted combretastatin A-4 analogues. Eur. J. Med. Chem. 125 (2017) 1098−1106.

[17] Q. Xu, M. Sun, Z. Bai, Y. Wang, Y. Wu, H. Tian, D. Zuo, Q. Guan, K. Bao, Y. Wu, W. Zhang. Design, synthesis and bioevaluation of antitubulin agents carrying diaryl-5,5-fused-heterocycle scaffold. Eur. J. Med. Chem. 139 (2017) 242−249.

[18] Q. Xu, Y. Wang, J. Xu, M. Sun, Tian H, Zuo D, Guan Q, Bao K, Wu Y, Zhang W. Synthesis and bioevaluation of 3,6-diaryl-[1,2,4]triazolo[4,3-*b*]pyridazines as antitubulin agents. ACS Med. Chem. Lett. 7 (2016) 1202−1206.

[19] N. Zhang, S. Ayral-Kaloustian, T. Nguyen, J. Afragola, R. Hernandez, J. Lucas, J. Gibbons, C. Beyer. Synthesis and SAR of [1,2,4]triazolo[1,5-a]pyrimidines, a class of anticancer agents with a unique mechanism of tubulin inhibition. J. Med. Chem. 50 (2007) 319−327.

[20] M. Driowya, J. Leclercq, V. Verones, A. Barczyk, M. Lecoeur, N. Renault, N. Flouquet, A. Ghinet, P. Berthelot, N. Lebegue. Synthesis of triazoloquinazolinone based compounds as tubulin polymerization inhibitors and vascular disrupting agents. Eur. J. Med. Chem. 115 (2016) 393−405.

[21] B. Zhang, Y.H. Li, Y. Liu, Y.R. Chen, E.S. Pan, W.W. You, P.L. Zhao. Design, synthesis and biological evaluation of novel 1,2,4-triazolo[3,4-b][1,3,4]thiadiazines bearing furan and thiophene nucleus, Eur. J. Med. Chem. 103 (2015) 335−342.

[22] F. Yang, L.Z. Yu, P.C. Diao, X.E. Jian, M.F. Zhou, C.S. Jiang, W.W. You, W.F. Ma, P.L. Zhao. Novel[1,2,4]triazolo[1,5-a]pyrimidine derivatives as potent antitubulin agents: design, multicomponent synthesis and antiproliferative activities. Bioorg. Chem. 92 (2019) 103260. doi: 10.1016/j.bioorg.2019.103260.

[23] H. Chen, S. Deng, Y. Wang, N. Albadari, G. Kumar, D. Ma, W. Li, S.W. White, D.D. Miller, W. Li. Structure-activity relatironship study of novel 6-aryl-2-benzoyl-pyridines as tubulin

polymerization inhibitors with potent antiproliferative properties. J. Med. Chem. 63 (2020) 827−846.

[24] S. Elmeligie, N.A. Khalil, E.M. Ahmed, S.H. Emam. New 3-substituted-2-(4-hydroxyanilino) pyridine derivatives: synthesis, antitumor activity, and tubulin polymerization inhibition. Arch. Pharm. Chem. Life Sci. 350 (2017), e1600256.

[25] M.C. Tuma, A. Malikzay, X. Ouyang, D. Surguladze, J. Fleming, S. Mitelman, M. Camara, B. Finnerty, J. Doody, E.L. Chekler, P. Kussie, J.R. Tonra. Antitumor activity of IMC-038525, a novel oral tubulin polymerization inhibitor. Transl. Oncol. 3 (2010) 318−325.

[26] C.M. Rudin, A. Mauer, M. Smakal, R. Juergens, S. Spelda, M. Wertheim, A. Coates, E. McKeegan, P. Ansell, X. Zhou, J. Qian, R. Pradhan, B. Dowell, A. Krivoshik, G. Gordon. Phase I/II study of pemetrexed with or without ABT-751 in advanced or metastatic non-small-cell lung cancer. J. Clin. Oncol. 29 (2011) 1075−1082.

[27] C. Le Manach, T. Paquet, C. Brunschwig, M. Njoroge, Z. Han, D. Gonzàlez Cabrera, S. Bashyam, R. Dhinakaran, D. Taylor, J. Reader, M. Botha, A. Churchyard, S. Lauterbach, T.L. Coetzer, L.M. Birkholtz, S. Meister, E.A. Winzeler, D. Waterson, M.J. Witty, S. Wittlin, M.B. Jiménez-Díaz, M. Santos Martínez, S. Ferrer, I. Angulo-Barturen, L.J. Street, Chibale K. A novel pyrazolopyridine with in vivo activity in plasmodium berghei- and plasmodium falciparum-infected mouse models from structure-activity relationship studies around the core of recently identified antimalarial imidazopyridazines. J. Med. Chem. 58 (2015) 8713−8722.

[28] P.R. Clarke, L.A. Allan. Cell-cycle control in the face of damage−a matter of life or death. Trends Cell Biol. 19 (2009) 89−98.

[29] Y.N. Liu, J.J. Wang, Y.T. Ji, G.D. Zhao, L.Q. Tang, C.M. Zhang, X.L. Guo, Z.P. Liu. Design, synthesis, and biological evaluation of 1-methyl-1,4-dihydroindeno[1,2-c]pyrazole analogues as potential anticancer agents targeting tubulin colchicine binding site. J. Med. Chem. 59 (2016) 5341−5355.

[30] Sybyl 7.3, Tripos Inc., 1699 South Hanley Road, St. Louis, MO 63144, U.S.A.

[31] R.B.G. Ravelli, B. Gigant, P.A. Curmi, I. Jourdain, S. Lachkar, A. Sobel, M. Knossow. Insight into tubulin regulation from a complex with colchicine and a stathmin-like domain. Nature, 428 (2004) 198−202.

[32] W.L. DeLano, DeLano Scientific, San Carlos, CA, USA, http://www.pymol.org, 2002.

Highlights

• 29 novel 3,6-diaryl-[1,2,4]triazolo[4,3-a]pyridines were synthesized. • **7i** dispayed an IC_{50} of 0.012 nM on HeLa and high selectivity over normal human cell HEK-293. • **7i** possessed potent antitubulin activity with a value similar to CA-4 (3.4 and 4.2 μM, respectively) • **7i** caused cell cycle arrest and apoptosis and disrupted microtubule networks.

Declaration of interests

☒ The authors declare that they have no known competing financial interests or personal relationships that could have appeared to influence the work reported in this paper.

☐The authors declare the following financial interests/personal relationships which may be considered as potential competing interests: